

# Molecular PET/CT Imaging-Guided Radiation Therapy Treatment Planning<sup>1</sup>

Habib Zaidi, PhD, PD, Hansjörg Veves, MD, Michael Wissmeyer, MD

The role of positron emission tomography (PET) during the past decade has evolved rapidly from that of a pure research tool to a methodology of enormous clinical potential. <sup>18</sup>F-fluorodeoxyglucose (FDG)-PET is currently the most widely used probe in the diagnosis, staging, assessment of tumor response to treatment, and radiation therapy planning because metabolic changes generally precede the more conventionally measured parameter of change in tumor size. Data accumulated rapidly during the last decade, thus validating the efficacy of FDG imaging and many other tracers in a wide variety of malignant tumors with sensitivities and specificities often in the high 90 percentile range. As a result, PET/computed tomography (CT) had a significant impact on the management of patients because it obviated the need for further evaluation, guided further diagnostic procedures, and assisted in planning therapy for a considerable number of patients. On the other hand, the progress in radiation therapy technology has been enormous during the last two decades, now offering the possibility to plan highly conformal radiation dose distributions through the use of sophisticated beam targeting techniques such as intensity-modulated radiation therapy (IMRT) using tomotherapy, volumetric modulated arc therapy, and many other promising technologies for sculpted three-dimensional (3D) dose distribution. The foundation of molecular imaging-guided radiation therapy lies in the use of advanced imaging technology for improved definition of tumor target volumes, thus relating the absorbed dose information to image-based patient representations. This review documents technological advancements in the field concentrating on the conceptual role of molecular PET/CT imaging in radiation therapy treatment planning and related image processing issues with special emphasis on segmentation of medical images for the purpose of defining target volumes. There is still much more work to be done and many of the techniques reviewed are themselves not yet widely implemented in clinical settings.

**Key Words.** Molecular imaging; PET/CT; radiation therapy; treatment planning; segmentation.

© AUR, 2009

Advances in genomics, proteomics, and biomedical technology are changing the practice of medicine in a profound way (1,2). The role of positron emission tomography (PET) during the past decade has evolved rapidly from that of a pure research tool to a methodology of enormous clinical potential (3). <sup>18</sup>F-fluorodesoxyglucose (FDG)-PET is widely used in the diagnosis, staging, and assessment of tumor response to therapy, since metabolic changes generally precede the more conventionally measured parameter of change in tumor size.

Data accumulated rapidly during the last decade to validate the efficacy of FDG-PET imaging in a wide variety of malignant tumors with sensitivities and specificities often in the high 90 percentile range. Although molecular PET/CT imaging is an obvious choice, the design of specific clinical protocols is still under development. The tracers or combinations of tracers to be used (eg, for imaging metabolism, hypoxia, and cell proliferation), when and how the imaging should be done after therapy, the selection of optimal acquisition and processing protocols, and robust algorithms for accurately performing quantitative or semiquantitative analysis of data are still undetermined. Moreover, each tumor-therapy combination may need to be independently optimized and validated. There have been multiple studies that have demonstrated the role of PET/CT especially for oncologic applications (4–6). It should be emphasized that much worthwhile research was carried out. However, there

*Acad Radiol* 2009; 16:1108–1133

<sup>1</sup> Divisions of Nuclear Medicine (H.Z., M.W.) and Radiation Oncology (H.V.), Geneva University Hospital, CH-1211 Geneva 4, Switzerland. Received December 24, 2008; accepted February 19, 2009. Supported by the Swiss National Science Foundation under grant SNSF 3152A0-102143. **Address correspondence to:** H.Z. e-mail: [habib.zaidi@hcuge.ch](mailto:habib.zaidi@hcuge.ch)

© AUR, 2009

doi:10.1016/j.acra.2009.02.014

are still many open questions offering many opportunities for future research.

Dual-modality techniques offer a critical advantage over separate computed tomography (CT) and PET scanning in correlating functional and anatomical images without moving the patient (other than table translation). Different designs of combined PET/CT scanners were developed for diagnostic purposes in clinical oncology and have been commercially available since the beginning of this century (7). This technique thereby produces anatomical and functional images with the patient in the same position and during a single procedure, which simplifies the image registration and fusion processes (8). In seeking to achieve accurate registration of the anatomical and functional data, dual-modality imaging offers several potential advantages over conventional imaging techniques. First, the PET and x-ray CT images are supplementary and complementary. PET images can identify areas of disease that are not apparent on the CT images alone (9). The latter provide an anatomical context that interpreters use to differentiate normal radiotracer uptake from that indicating disease and to help localize disease sites within the body. Second, the low noise x-ray CT data can be used to generate a patient-specific map of attenuation coefficients and other a priori anatomical data, which in turn are used to correct the PET emission data for errors from photon attenuation (10), scattered radiation (11), and other physical degrading factors such as partial volume effect (12). In these ways, the CT images can be used to improve both the visual quality and the quantitative accuracy of the correlated radiotracer data (13).

In parallel, radiation therapy (RT) has gone through a series of revolutions in the last two decades, now offering the possibility to produce highly conformal radiation dose distribution by using techniques such as intensity-modulated radiation therapy (IMRT) using tomotherapy, volumetric modulated arc therapy, and many other RT units for dose painting. The improved dose conformity and steep dose gradients have necessitated enhanced patient localization and beam targeting techniques for radiotherapy treatments (14). Components affecting the reproducibility of target position during and between subsequent fractions of RT include the displacement of internal organs between fractions and internal organ motion within a fraction. Image-guided radiation therapy (IGRT) uses advanced imaging technology to better define the tumor target and is the key to reducing and ultimately eliminating the uncertainties (15).

In general, anatomical cross-sectional images (CT and magnetic resonance imaging [MRI]) are used to delineate the treatment volumes, and radiation treatment portals are designed to entirely cover the planning treatment volume and deliver a uniform dose distribution to it. The ability of IMRT to deliver nonuniform dose patterns by design has raised the question of how to “dose paint” and “dose sculpt” (16,17).

In this regard, it was suggested that molecular imaging using PET/CT may be of additional value (18–23) even if the issue is still controversial (24,25). PET allows a more correct delineation of gross tumor volume (GTV) and planning target volume. It should, however, be emphasized that much scientific research and clinical studies are needed before this potential can be realized. The recent enthusiasm in the use of PET/CT-guided RT treatment planning is stimulated by the commercial availability of advanced imaging technologies and their incorporation in treatment planning software offering the possibility to integrate data from different departments and even from different hospitals into RT treatment planning (26). One of the main difficulties encountered by radiation oncologists is the delineation of the treatment volume from noisy PET data (13). Identification of lesion boundaries in general is not a trivial problem as whole-body images exhibit inhomogeneity (27). Another challenge for the industry is to provide an easy, open, and vendor-independent platform for incorporating the PET/CT information in a DICOM-compatible format into the RT dose planning software.

This review documents technological advancements in the field focusing on the conceptual role of molecular PET/CT imaging in RT treatment planning and related image processing issues with special emphasis on segmentation of PET images for the purpose of defining target volumes.

## PROGRESS IN RT TECHNOLOGY

Ionizing radiation has been a proven cancer therapy technique for more than a century (28,29). Steady technological advancement in imaging has led to continuing improvement and expanding applications of RT, allowing, among others a 3D guided target definition (30,31). Indeed, the passage from fluoroscopy to CT in the late 80s permitted to obtain a better definition of the target in 30%–70% of patients treated with RT (32). CT imaging has shifted the focus of treatment planning and guidance from inferring disease location based on radiographic bony landmarks to a more direct method of using soft tissue to define both the tumor target and the normal organs in 3D. This anatomically conformal approach attempts to maximally avoid normal tissues, to reduce the radiation induced toxicity and to enable dose escalation. A greater degree of flexibility is required in the case of target volumes close to sensitive organs, such as the salivary gland, optic nerves, or the spinal cord. This can be achieved by using a larger number of incident beams and by subdividing the beam area into a series of smaller beam segments. This approach began to emerge in the middle of the 1990s and is known as IMRT. IMRT is a logical evolution of the 3D conformal therapy approach. It enables the tumor to be treated with a uniform high dose of radiation while

decreasing the radiation received by the surrounding organs by using segments of varying intensity to sculpt a much tighter dose distribution around the target. This technique has been rapidly applied to almost all types of tumors and has demonstrated its utility (14). One of the known drawbacks of this technique is that it is time consuming (requires hours of manual tuning to determine an effective radiation treatment plan for cancer patients). Much worthwhile research is being carried out to automatically determine optimal radiation treatment plans (using, for example, machine learning, a subfield of artificial intelligence) in few minutes without compromising the quality of treatment (33).

Small brain tumors and certain benign brain disorders can be treated with stereotactic radiosurgery, which is based on a mechanical fixation frame adopted from neurosurgery applications. This provides an external 3D reference system to accurately localize the intracranial target. Despite its name, stereotactic radiosurgery is a nonsurgical procedure that uses highly focused x-rays to treat certain types of brain tumors. Stereotactic radiosurgery directs high doses of RT in a single session. When the treatment is applied in a small number of fractions, it is referred to as stereotactic RT. Stereotactic body RT (34) extends radiosurgery principles to disease throughout the entire body and imposes more stringent requirements on the accuracy and precision of treatment planning, patient positioning, and management of organ motion. It enables physicians to adjust the radiation beam based on the position of the target tumor and critical organs while the patient is in the treatment position.

There are essentially two approaches to account for tumor motion: minimization of target motion via immobilization, or alternatively to account for physiologic tumor motion via tracking or gating. Active or passive breath-hold techniques fix the tumor in a stable position for a short period. The beam is then activated when the breath is held with the proper tidal volume. Another immobilization approach uses abdominal compression that limits diaphragmatic excursion, and thereby the respiratory motion of the tumor. This substantially restricts tumor motion allowing for smaller treatment margins. Respiratory gating can reduce the deleterious effects of intrafraction motion (35) by synchronizing treatment with the patient's respiratory cycle (36–39).

Gating requires real-time assessment of the respiratory cycle, and activating the beam at a particular phase of the respiratory cycle (eg, end-inhale or end-exhale), while maintaining the radiation beam in a fixed position. Tracking usually involves the use of a surrogate for tumor motion, such as a fiducial marker. Both gating and tracking typically rely on a close reproducible relationship between the surrogate and tumor, although in the ideal situation the tumor would be directly visualized with image guidance (38). Similar developments have been carried out using combined PET/CT imaging considering that motion occurs because of respira-

tion, cardiac motion, peristalsis, and bladder filling, all of which can lead to motion blurring or misregistration errors between the PET and CT image acquisitions (40–47). Respiratory motion remains a major source of error in correct localization and accurate quantitation of lesion activity and treatment planning using combined PET/CT units.

It was reported in a study including 300 patients with proven liver lesions that approximately 2% appeared to have the lesion localized in the lung from respiratory motion (48). A more recent study examined 100 clinical PET/CT studies for the frequency and magnitude of misalignment at the diaphragm position between the CT and the PET data (49). There was a misalignment between the CT and the PET data in 50 patient studies (50% of cases). The misregistration was greater than 2 cm in 34% of cases whereas it was 2–4.5 cm in 3% of cases. Care therefore must be taken when interpreting results from patients with disease in periphery of the lung where noticeable radiotracer uptake may be contributed by respiratory-induced motion artifacts rather than disease.

In comparison to 3D-RT, four-dimensional RT requires very high accuracy in space and in time for tumor localization and needs IGRT (15,50,51). Four-dimensional RT is the explicit inclusion of the temporal changes in anatomy during the imaging, planning, and delivery of RT. New innovations in IGRT, such as cone-beam CT, are making this practical by acquiring CT images before each treatment to permit verification and adjustment of the target position. Robust and computationally efficient algorithmic design is the restrictive aspect in accomplishing highly accurate and precise dose delivery to the complex anatomy of cancer patients (52).

Existing radiation treatment delivery units for IGRT integrating patient immobilization and respiratory control devices, such as tomotherapy, the Novalis Shaped Beam Surgery unit (BrainLAB), CyberKnife, and many other devices are now commonly used in academic RT facilities. Tomotherapy (Tomotherapy Inc, Madison, WI) uses a rotational delivery and moving table approach so that the radiation beam follows a dynamic helical pattern (53,54). It is based on IMRT delivered throughout continuous 360° rotations using a binary multileaf collimator. RapidArc technology was recently introduced by one of the major vendors (Varian Medical Systems, Palo Alto, CA) to allow volumetric arc therapy thus delivering a precisely sculpted 3D dose distribution with a single full rotation of the linear accelerator (linac) gantry (55,56). It incorporates advanced capabilities such as variable dose-rate, variable gantry speed, and accurate and fast dynamic multileaf collimators, to optimize dose conformity, delivery efficiency, accuracy, and reliability (57).

BrainLAB uses a 6-MV linear accelerator with micro-multileaf collimators ranging in leaf widths from 3 to 5.5 mm. Two 2-keV orthogonal x-ray cameras reveal bony landmarks or implanted fiducial markers whose position is compared

with their expected position on digitally reconstructed radiographs generated from the CT simulation. The CyberKnife (Accuray) uses a frameless image-guided process to direct a lightweight linear accelerator mounted on a robotic arm along six spatial axes providing broader translational and rotational movement. Two orthogonal, diagnostic x-ray cameras are mounted on the ceiling and provide real-time imaging for tracking. Implanted fiducials or reliable bony landmarks are used to localize the tumor and deliver treatment in real time. Multiple isocenters can be used during one treatment.

Technological innovation continues to improve the accuracy and precision of RT. Heavy and light ions as well as proton beams have physical properties that can help to reduce normal tissue damage (58–61). Because of their mass, ions and protons interact intensively along their tracks and stop when they reach a depth related to their initial energy. Consequently, very little dose is deposited in normal tissues that lie beyond the target volume. Furthermore carbon ions offer biologic advantages owing to an increased relative biologic effectiveness within the Bragg peak region. This leads to improved dose distribution, permitting dose escalation within the target and avoiding radiation-induced injuries to critical organs. Therefore, RT with heavy charged particles such as protons and ions suggests a clinical gain in poorly radiosensitive tumors and tumors located close to critical organs such as the spinal cord. Potential indications include tumors with a low  $\alpha/\beta$  ratio such as chordomas, low-grade chondrosarcomas, and adenoid cystic carcinomas (62,63). Furthermore, it is beneficial in the treatment of pediatric diseases and in eye tumors (64–67). However, the cost associated with building the highly sophisticated infrastructures required and the daily operation of proton and ion beam treatment facilities limited their use to a few centers worldwide. Nevertheless, proton therapy has lately become more and more popular and new proton treatment centers have been recently established and others are planned in various places around the world.

The selective energy deposition of heavy ion therapy has led to a growing interest in quality assurance techniques for dose verification such as “in-beam” PET (68). Owing to the current lack of commercial solutions in the beginning, various “in-beam” PET (69–71) and, later, PET/CT (72,73) systems have been developed or assessed in academic settings. In particular, the challenges posed by this unconventional application of PET and PET/CT involving low count rates that are orders of magnitude lower than those encountered in diagnostic imaging since the signal of interest is comparable to the noise originating from the intrinsic radioactivity present in current lutetium orthosilicate; lutetium yttrium orthosilicate (LSO/LYSO) detectors is also worth mentioning (73). Despite the promising results obtained so far for dose verification using PET, it is unlikely that future commercial radiation therapy units will include dedicated PET systems as a key component

of such systems considering the cost and complexity of the technology. History showed that industry is willing to translate these research advances into commercial products only if the benefits conveyed to patients by any new technology are clinically proven as demonstrated by improvements in health outcomes with an acceptable level of patient cost-effectiveness. Operating such units requires extensive technical and organizational efforts that may restrict its use to academic centers having the required scientific and technical resources.

More recently, a novel hybrid MRI-linac technology combining a linac and MRI system on the same gantry was developed. The system comprises a 6-MV linac mounted on the open end of a biplanar, low field (0.2 T) MRI magnet on a single gantry having the capability to freely rotate around the patient (74). The opening between the planes of the biplanar MRI system is about 27 cm, large enough for a head. The system was designed in such a way to avoid mutual magnetic and radiofrequency interferences allowing for a real-time MRI while irradiated by the linac. The first images generated using this system in December 2008 for proof of principle demonstrated that the MRIs during 6-MV irradiation do not show significant distortions and are very similar to those obtained before irradiation, although a small difference in signal-to-noise ratio between images was reported.

### ADVANCES IN ANATOMOLECULAR PET/CT IMAGING INSTRUMENTATION

In late 1980s and early 1990s, investigators from the University of California, San Francisco, led by late Dr. B. Hasegawa pioneered the development of a hybrid single-photon emission computed tomography (SPECT)/CT device which could record both SPECT and x-ray CT data for correlated functional/structural imaging using an array of semiconductor (HPGe) detectors (75). Later, Dr. Townsend and coworkers (University of Pittsburgh) pioneered in 1998, the development of combined PET/CT imaging systems. These have the capability to record both PET emission and x-ray CT data for correlated functional/structural imaging (76). This hybrid unit consists of two separate devices, namely a PET and a CT scanner, linked by one common bed and workstation console where data from both modalities are acquired sequentially rather than simultaneously as planned during the earlier conceptual design of the machine (77). Both the CT component and the PET detectors were mounted on opposite sides of the rotating stage of the CT system and imaged a patient with a common patient table translated between the centers of the two tomographs which are offset axially by 60 cm. The PET/CT system had a specially designed patient table that was designed to minimize deflection when it is extended into the patient port. The PET/CT prototype was operational at the University of Pittsburgh between May 1998 and August 2001,

during which more than 300 cancer patients were scanned (78). The success of these initial studies prompted significant interest from the major medical imaging equipment manufacturers who have introduced commercial PET/CT scanners for clinical use since the beginning of the 21st century.

Modern commercially available dedicated cylindrical full-ring PET tomographs are still considered to provide state-of-the-art performance for whole-body scanning (79) whereas various geometries were suggested for dedicated high resolution brain (80), female breast (81,82) and prostate (83) scanning. There is also a renewed interest in old technologies such as time-of-flight PET thanks to the development of faster scintillation crystals and electronics that made this approach feasible on commercial clinical systems (84,85). On the other hand, despite the concerns raised regarding radiation exposure particularly to children (86), the progress in CT technology has been immense during the last two decades allowing the introduction of CT scanners with up to 256 (87) and even 320 (88) slice capability and many novel technologies such as dual-source CT, C-arm flat-panel-detector CT and micro-CT (89,90).

Commercial PET/CT systems are usually configured by designing a gantry that mounts a stationary PET detector ring in tandem with a platform that rotates the CT imaging chain around the patient using a mechanical configuration similar to that used in a conventional diagnostic CT scanner. The CT study typically is used for both localization of the tracer uptake as well as for attenuation correction of the PET data set. In these ways, the CT data can be used to improve both the visual quality and the quantitative accuracy of the correlated PET data. Current commercial PET/CT systems consist of multislice spiral CT of up to 64 slice capability, thus allowing cardiac imaging to be performed with a high temporal resolution. In addition, the use of CT for attenuation correction of the corresponding PET data increases patient throughput by approximately 30% in comparison to conventional radionuclide transmission sources (91). However, CT also increases patient dose and despite the significant progress achieved in CT-based attenuation correction during the last decade, some problematic issues still remain open research questions and are being investigated by many active research groups (10,92).

The advent of combined PET/CT units is a prominent example of advance in molecular imaging technology that offers the opportunity to modernize the practice of clinical oncology by improving lesion localization and facilitating treatment planning for RT (7). There are, however, several important challenges that must be overcome. This includes appropriate handling of potential artifacts that may arise due to effects such as respiratory-induced misregistration of the PET and CT data, truncation artifacts owing to discrepancy between fields of view in a dual-modality system, the presence of oral and intravenous contrast medium, artifacts from

metallic implants, beam hardening artifacts caused by the polychromatic nature of CT x-rays, x-ray scatter in CT images for future generation cone-beam geometries, and other CT artifacts from any source (10,93).

The major area of clinical use of PET/CT is in oncology, where the most commonly used radiopharmaceutical is  $^{18}\text{F}$ -FDG. FDG-PET has already had a huge valuable outcome on cancer treatment and its use in clinical oncology practice continues to develop (5,6,94). The advantages of combining morphological and functional imaging (compared to PET or CT alone) have been clearly demonstrated by numerous publications for a wide variety of applications (78,95–97). There is an abundant literature reporting patient studies where the combined PET/CT images provided additional information, thus impacting the characterization of abnormal FDG uptake and influencing patient management (4–6,94).

As diagnostic techniques transition from the systems to the molecular level, the role of multimodality imaging becomes ever more important. Even if the combination of PET and MRI in a single gantry to enable truly simultaneous acquisition is technically challenging owing to the strong magnetic fields, this technology will allow to bridge the gap between molecular and systems diagnosis. Both imaging modalities offer richly complementary information about disease; their integration into a combined system offering simultaneous acquisition will capitalize the strengths of each, providing a hybrid technology that is significantly better than to the sum of its parts (98). The recent introduction of hybrid PET/MRI technology is considered by many experts as a major breakthrough that will potentially lead to a revolutionary paradigm shift in healthcare and revolutionize clinical practice (99). Several active research groups in academic and corporate settings are focusing on the development of various configurations of MRI-compatible PET inserts to allow simultaneous scanning using the most highly sophisticated molecular imaging technologies available today (100). Significant progress has been made resulting in the design of few preclinical PET/MRI scanners and one human prototype (BrainPET) dedicated for simultaneous PET/MRI brain imaging (101).

The BrainPET PET/MRI system is being assessed in a clinical setting and could indeed be used for delineation of brain tumors for RT treatment planning. The feasibility of MRI-guided attenuation correction (102–104) and the prospective applications of a whole-body PET/MRI system are under way (105–108). Such a system, when available, could certainly be a valuable tool for PET/MRI-guided RT treatment planning, particularly for localizations where the tumors are better visualized on MRI as compared to CT owing to the high soft-tissue contrast. Another advantage inherent to the modality is the possibility to perform MRI spectroscopy to measure the regional biochemical content and to assess

metabolic status or the presence of neoplasia and other diseases in specific tissue areas (109).

### PROGRESS IN NEW CANCER-SPECIFIC PET PROBES

The introduction of FDG and a multitude of novel probes have clearly demonstrated the enormous potential of nuclear medicine as an emerging discipline in the field of molecular imaging (110,111). It can arguably be stated that FDG-PET, as a single modality, has made an everlasting impact on the specialty of nuclear medicine. In fact, it has rejuvenated the field and has changed its image in the medical community. It is not an exaggeration to speculate that in the coming years, the number of FDG-PET images performed in most facilities will exceed that of all other procedures performed with radiolabeled compounds. This recognition led our distinguished colleague Henry Wagner to name FDG as the "Molecule of the Century" because of its unequalled impact on the evolution of the specialty of nuclear medicine.

Oncological PET probes (other than FDG) can be broadly categorized into three groups: those labeled with  $^{18}\text{F}$ ,  $^{11}\text{C}$ , and other tracers (112). Fluorine-18 and  $^{11}\text{C}$  can be used to label with different amino acids, substrates involved in fatty acid synthesis, protein synthesis, amino acid transport substrate and tracers related to nucleic acid synthesis. The same radionuclides can also be labeled with specific ligands for receptor imaging (ie, estrogens, dihydrotestosterone, or somatostatin). Many other radiotracers can be labeled with  $^{68}\text{Ga}$ ,  $^{60}\text{Cu}$ , or  $^{64}\text{Cu}$  that target cell hypoxia, bone metabolism, and receptors. Some of these tracers with more specific mechanism of uptake have shown potential and seem promising particularly in some cancers where conventional FDG imaging has limited role (113).

The recent progress in the development of tracers targeted to other aspects of tumor biology, including cell growth, cell death, oncogene expression, drug delivery, and tumor hypoxia will significantly enhance the capability of clinical scientists to differentiate tumors and are likely to be used to guide treatment decisions. The contribution of PET to understanding the clinical biology of cancer and to guiding targeted, individualized therapy will continue to grow with these new developments (4,114).

Several new tracers are expected to be approved and routinely used in the coming years. Agents that measure regional hypoxia in malignant tumors (eg,  $^{18}\text{F}$ -FMISO,  $^{18}\text{F}$ -2-(2-nitro-(1H-imidazol-1-yl)-N-(2,2,3,3,3-pentafluoropropyl)-acetamide (EF5),  $^{60}\text{Cu}$ -ATSM) (115–118) and possibly in some benign disorders will be more frequently employed (119). Hypoxia is considered the main factor in lack of response following radiation or chemotherapy. Therefore, in patients with hypoxia, radiation, or chemotherapy may be postponed

until optimal oxygen levels have been restored in the tumor. In certain cancers,  $^{18}\text{F}$ -labeled fluorothymidine may prove to be of value in monitoring response to therapy instead of FDG (120). This tracer, however, does not appear optimal for diagnostic purposes because it is insensitive for detecting slow growing tumors.  $^{18}\text{F}$ -labeled DOPA is being used for the diagnosis of Parkinson's disease (121) and will be more widely adopted as a diagnostic tool for the imaging of neuroendocrine tumors (122,123).  $^{68}\text{Ga}$ -labeled DOTA octreotide and  $^{124}\text{I}$ -labeled MIBG also appear to have the promise of improving the management of patients with neuroendocrine tumors. Peptides containing amino acid sequence arginine-glycine-aspartate appear to have an affinity toward integrins that are present on activated endothelial cells in tumors with angiogenesis (124).  $^{18}\text{F}$ -galacto-arginine-glycine-aspartate is a tracer developed for specific imaging of  $\alpha_v\beta_3$  expression, a receptor involved in angiogenesis and metastasis that proved to be particularly useful in patients with squamous cell carcinoma of the head and neck (125). This probe might be used for the evaluation of angiogenesis and for planning and response evaluation of  $\alpha_v\beta_3$ -targeted therapies. Estrogen receptor targeting agents may be used to assess noninvasively, the estrogen receptor section of tumors in vivo by  $^{18}\text{F}$ -labeled estrogen analogues such as fluoestradiol (126). Angiogenesis, the formation of new vessels is the target of a multitude of novel therapies and drugs. Therefore, direct visualization of this biologic response to tumor hypoxia and cell proliferation will be of great importance in developing these drugs. Apoptosis or programmed cell death can be imaged with radiolabeled Annex V to monitor response to therapy in cancer (127). Many other tracers are being investigated for various applications that might translate in new clinical applications. Our belief is that it is the power of molecular imaging using highly specific tracers that is central and not the number of slices of the CT subsystem when considering the example of combined PET/CT (2).

### MOLECULAR PET/CT IGRT TREATMENT PLANNING

Early attempts to use nuclear medicine and particularly PET for RT were described in the late 1990s by few groups (128–135). This was further stimulated and put into perspective after the introduction of the concept of biological imaging (136). Thereafter, the technical aspects of PET/CT-based RT were described in many reports and state-of-the-art reviews (18,22,137–140).

The fundamental motivation for the use of PET/CT in radiation therapy is that it provides better visualization than CT simulation in the sense that in some cases CT misses some areas that light up on the PET study or that the lesion volume is in reality smaller on the PET/CT study than on the

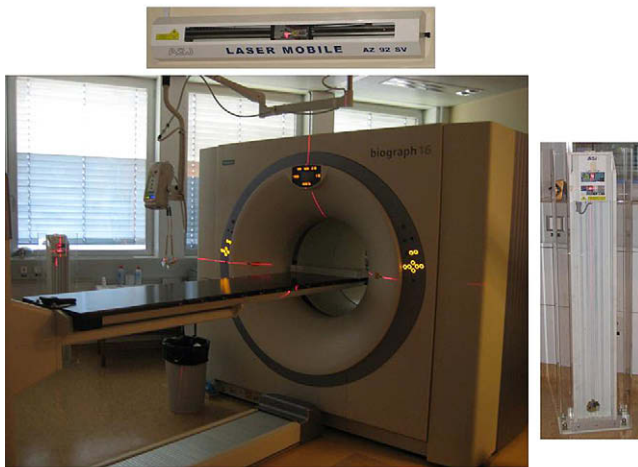


**Figure 1.** Photograph of the Biograph 16 HI-REZ PET/CT scanner (Siemens Medical Systems, Erlangen, Germany) installed at Geneva University Hospital and used routinely for radiation therapy simulation and positron emission tomography/computed tomography–based treatment planning. The scanner is equipped with a flat-panel tabletop and external room lasers. The 70 cm large diameter bore allows most patients to be imaged in the treatment position with the use of suitable immobilization devices.

CT alone. In addition, discrepancies between CT and/or MRI and PET findings are very often reported in the literature (20,21,52,138,141–148). Both state-of-the-art FDG-PET and novel PET probes' applications in the process of RT treatment planning are reviewed below.

### Current Evidence of FDG-PET/CT Utilization in Target Volume Definition

Molecular imaging of tumor metabolism using FDG-PET has shown high sensitivity, specificity, and accuracy in a variety of malignancies, such as head-and-neck cancer, lung cancer, esophageal cancer, breast cancer, colorectal cancer, lymphoma, and malignant melanoma. Evolving areas for the diagnostic use of FDG-PET are differentiated thyroid carcinoma, gastropancreatic tumors, cholangiocarcinoma, gynecologic tumors, bladder cancer, and malignancies of the bone and soft tissues (6).

With the possibility to image tumor metabolism, the idea of “biologic” target volume in addition to the well known GTV and clinical target volume concepts arose to include tumor biology into the treatment planning (149). The first studies dealing with FDG-PET–based target volume definition have been published in the late 1990s (128–133). Today, there are more than 1000 PUBMED entries when searching for “*FDG PET*” AND “*Radiotherapy*.”

Not only having direct impact on target volume delineation, FDG-PET led to a significant change in the therapeutic approach between curative and palliative and vice versa in 10%–30% of the cases due to detection of distant metastases

or different local extension when compared to other imaging modalities (143,150–154). Additionally, inter- and intra-observer variability was considerably reduced when PET information was available for target volume delineation (154–157).

With the commercial availability of multislice hybrid PET/CT scanners of the last generation equipped with fixed RT positioning laser systems in the scanner room, a “one-stop shop” providing diagnostic PET/CT and RT planning CT scan in only one session has become possible and is being routinely used in many institutions (Figure 1). Thus, nowadays more and more studies deal with PET/CT-based planning, as 3D image fusion software has become widely available in the clinic. Commercial software also offer simple and reliable tools compared to the “early times” where studies were obtained on different scanners and fused mentally or manually. Different PET image segmentation techniques have been devised and applied resulting in significant changes in target volumes in up to 50% of the patients when compared to CT-based simulation (158–161).

These findings are encouraging but need to be confirmed by prospective studies before PET/CT-guided RT can be used with confidence in clinical routine. There are a few drawbacks that hindered the widespread application of FDG-PET/CT in target volume determination in RT: 1) the number of patients included in published reports is in most cases small, 2) limited or absence of correlation with histology, 3) the heterogeneity of the methods applied in target volume delineation, and 4) missing information regarding the outcome of treated patients, which is not surprising given that the use of “biologic” target volume in target volume delineation has started only a few years ago (Table 1). Other potential problems of PET/CT-based target volume delineation, such as data transfer and compatibility between imaging systems and RT planning software, patient or organ motion, partial volume effects, and thresholds for significant metabolic activity are discussed in the following sections.

#### *Head-and-neck Tumors*

Feasibility of FDG-PET/CT–based target volume delineation for conformal 3D treatment and even IMRT in head and neck tumors has been reported by various authors (137,162,163). Geets et al reported that the use of pretreatment FDG-PET and per-treatment CT or MRI significantly impacts the delineation of target volumes in pharyngo-laryngeal squamous-cell carcinoma, resulting in more normal tissue sparing after conformal RT planning (164). In addition, PET might help to identify primary tumors associated with metastases where structural imaging has limited detection capabilities (Figure 2). The same group compared standard imaging techniques and PET findings with the pathologic specimen from larynx cancer (165). They did not find relevant differences between CT and MRI, but reported significantly smaller target volumes when drawn

**Table 1**  
**Summary of Recent Contributions Assessing the Impact of PET/CT on Target Volume Definition in FDG Avid Malignancies**

Localization	Reference	n	Reference Modality	GTV Delineation Method	Impact of PET on GTV	Other Important Findings
Head and neck	(164)	18	CT and MRI	Manually: CT and MRI	Significant reduction of target volumes (up to 18%)	Significant reduction of mean dose to ipsilateral (31%) and contralateral (11%) parotids
	(319)	38	CT	Automated: PET Manually: CT and PET/CT	Significant change of GTV, no significant change of PTV	
	(320)	22	CT	Manually: CT, PET and fused PET/CT	Significant change of GTV	Change of TNM stage in 22%
	(321)	20	CT	Manually: CT and fused PET/CT	No significant differences between GTV CT and GTV PET/CT	Significantly higher interobserver agreement for GTV PET/CT when compared to GTV CT
	(322)	16	CT	Manually on CT and fused PET/CT	Higher interobserver variability for GTV PET/CT than GTV CT	
	(274)	25	CT	CT: manually	Significantly higher interobserver concordance for GTV PET/CT than for GTV CT	
				PET/CT: manually based on halo phenomenon		
Esophageal cancer	(323)	21	CT	Manually: PET and CT	Median 38% of GTV-PET not covered by GTV-CT	Clinical stage altered in 8/21 patients (38%); change of intent (curative -> palliative) in 5/21 patients (24%)
	(324)	16	CT	Manually: CT and PET/CT	Smaller GTV in 62.5%	
	(325)	25	CT, EUS	Manually: CT and PET/CT	GTV PET < GTV CT	EUS detected significantly more patients with locoregional lymphadenopathy
	(326)	10	CT	Manually: CT and PET/CT	NA	Reduced intra- and interobserver variability when adding the PET information
						Interobserver variability significantly improved (up to 84%) by adding the PET information
NSCLC	(160)	19	CT	Halo phenomenon	Up to 25% GTV modification in 10/19 patients. (52%)	Better correlation between real tumor volume and PET/CT than PET or CT alone
	(327)	52	Pathologic specimen; CT	NA	NA	Major GTV changes based on inclusion or exclusion of lymph nodes
	(171)	21	CT	Manually	Significant changes of CTV in 55%	Significant dose escalation possible while respecting dose constraints for organs at risk
	(328)	21	CT	Manually	Significant changes of GTV in 67%	

**Table 1**  
**(Continued)**

Localization	Reference	n	Reference Modality	GTV Delineation Method	Impact of PET on GTV	Other Important Findings
	(155)	33	CT	Manually and automated (source to background ratio)	GTV PET/CT smaller than GTV CT	Reduced interobserver variability using automatic GTV delineation; PET/CT best correlated with pathology
	(329)	21	CT	Manually: CT and fused PET/CT	Significant change in 39%	TNM staging modified in 48%; Change of treatment modality (curative -> palliative) in 14%
Breast cancer (tumor bed)	(330)	12	CT	Manually: CT and PET	PTV PET greater than PTV CT (median volume ratio: 1.16)	Inadequate coverage of PET/CT based GTV by CT PTV in 9/12 patients (75%)
Breast cancer (axilla)	(208)	15	CT	Manually: CT and PET	Increase of axillary dose in 11/13 patients (85%) when adding PET information	
Cervical cancer	(331)	51	CT	Manually: CT and PET/CT	Discordant CTV between PET and CT in 37% of patients	According to PET more extensive nodal involvement in 27% of patients
	(332)	11	Intracavitary brachytherapy planning	Manually: PET	Significantly better dose coverage of the tumor without significant dose increase to bladder and rectum	
Hodgkin lymphoma	(198)	30	CT	Manually: CT and PET	Increase of target volumes of 8–87% in 7/30 patients (23%); decrease of target volume of 18 and 30% in 2/30 patients (7%)	
Rectal cancer	(193)	20	CT	Manually: CT and PET/CT	Mean GTV PET/CT < GTV CT; PTV altered by PET/CT in 17%	Change of treatment fields and patient management in 26%
	(333)	25	CT	Manually: fused PET/CT	PET/CT-GTV significantly greater (mean 25.4%) than CT-GTV	Clinical stage or treatment purpose altered in 4/25 patients (24%)

PET, positron emission tomography; CT, computed tomography; FDG, fluorodeoxyglucose; GTV, gross tumor volume; MRI, magnetic resonance imaging; EUS, endoscopic ultrasound; GTV, gross tumor volume; CTV, clinical target volume.

The number of patients (n) enrolled in the study protocol, impact of PET on GTV delineation and other important findings are also given.

on FDG-PET. In addition, PET-based tumor volumes showed better correlation with pathologic findings compared with CT, both for the primary tumor and the locoregional lymph nodes (165). However, all imaging techniques partially underestimated the macroscopic tumor extension when compared to pathology. These findings have been confirmed recently by Burri et al (166).

Van Baardwijk et al showed in their review (167) that in four of six studies with a total of 139 patients, the GTVs drawn on PET/CT were significantly smaller than those drawn on CT only. One of the first articles evaluating clinical outcome following PET/CT-guided RT in head-and-neck

cancer showed favorable 3-year overall state and disease-free survival rates (168).

*Lung Cancer*

Besides head-and-neck tumors, FDG-PET based target volumes are well documented in non-small-cell lung cancer. This is probably because staging of lung cancer is one of the most important and well established indications for FDG-PET with a known high diagnostic accuracy and documented impact on clinical decision making (169). Its high sensitivity and specificity for lymph node involvement (Figure 3) and the capacity to better discriminate between



**Figure 2.** Patient with stage IIA Hodgkin lymphoma. The gross tumor volumes delineated on the positron emission tomography/computed tomography (PET/CT) scan is shown in green color. PET revealed an additional 7 mm paratracheal lymph node (*arrow*) that was missed on CT.

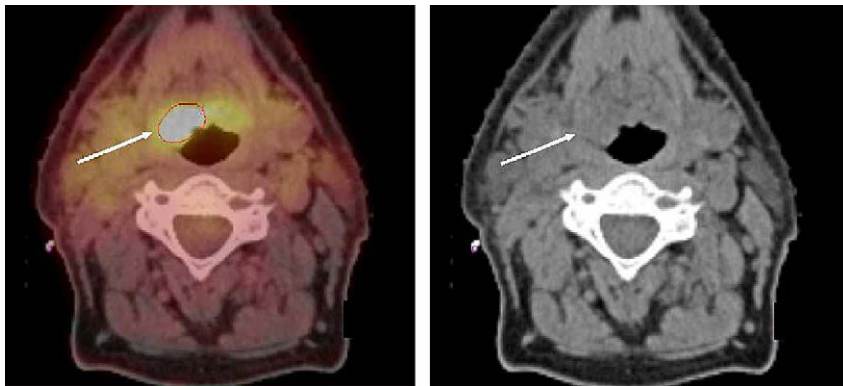


**Figure 3.** Patient with cervical lymph node metastases of squamous cell carcinoma from an unknown primary tumor. The gross tumor volume delineated on the positron emission tomography/computed tomography scan (*red color*) revealed the primary tumor located on the base of tongue (*arrow*) that was not identified on diagnostic magnetic resonance imaging, computed tomography, and panendoscopy.

tumor extent and atelectasis may substantially alter the target volumes (95,133,170–172). One such example is shown in Figure 4 where PET allowed excluding associated atelectasis that was impossible to differentiate using CT alone. In addition, several groups have shown the potential of FDG-PET to either reduce radiation burden to organs at risk or to considerably increase the dose delivered to the tumor (141,173). Furthermore, lung cancer is the first entity, in which early state outcome studies have shown that PET/CT based target volume delineation did not lead to a significantly higher number of in or out of field tumor recurrences when compared to standard CT-based target volume delineation (174,175). Overall, in most studies a significant change of target volumes was found in 25%–50% of the patients when PET information was added to the planning algorithm. The observed change in volume was about 20%–25%.

However, the lung is an organ largely susceptible to motion artifacts, leading to potential overestimation of large lesions and underestimation (partial volume effects) of small lesions that need to be taken into account when drawing target volumes (144,176,177). In addition, up to now, no consensus exists on which segmentation technique has to be used to define the metabolic margins of a non–small-cell lung cancer lesion (178,179).

#### *Esophageal Cancer*

Compared to CT, PET alone showed higher specificity but lower sensitivity for detection of lymph node involvement, whereas PET/CT could at least partially compensate this drawback (180–182). Therefore, PET has shown its capacity to enlarge the target volume beyond CT volumes when showing lymph node metastases in unexpected locoregional

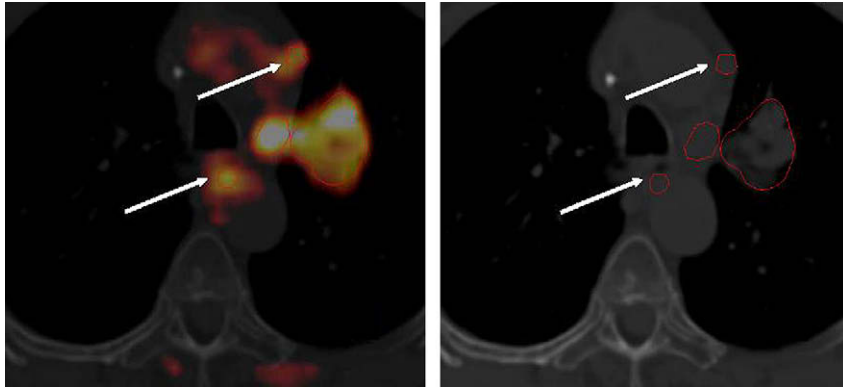


**Figure 4.** Patient with poorly differentiated carcinoma of the left lung. Fused positron emission tomography/computed tomography (CT) images detected two additional  $^{18}\text{F}$ -fluorodeoxyglucose positive mediastinal lymph nodes of 6 mm. The diagnostic CT scan performed on the same day did not classify these lymph nodes as suspicious.

regions (183,184). However, PET/CT-guided RT is not recommended in esophageal cancer owing to its low sensitivity.

#### *Gynecological Tumors*

Recent studies have proven the value of FDG-PET/CT for locoregional and distant staging of cervical cancer with a high sensitivity and specificity (185–188), especially in the detection of para-aortal and pelvic lymph node metastases which might be included in the target volume. First small series have shown feasibility and considerable impact of FDG-PET/CT-based target volume delineation on both conformal and IMRT planning (189). Additionally, PET was shown to provide valuable additional information for brachytherapy planning in patients with various gynecological cancers (158,190,191). Very few clinical data on the use of FDG-PET in RT treatment planning of gynecological tumors other than cervical cancer are available as of today.

#### *Rectal Cancer*

In colorectal cancer, the problem is inverse because PET provides excellent sensitivity (100%) but poor specificity (43%), most probably due to local inflammatory processes. However, metabolic information especially about small locoregional lymph nodes and distant metastases is crucial to determine stage appropriate treatment of the patients (eg, “down-staging” by radiochemotherapy before curative surgery) (192). This can result in significant changes in treatment fields and patient management (193). Additionally, FDG-PET might be useful in IMRT planning with dose escalation using dose painting targeted to highly metabolic regions of the tumor. Two studies with a total of 46 patients showed significantly increased target volumes when adding the information provided by PET to the morphologic CT images (152,158).

#### *Lymphoma*

With its known high sensitivity and specificity in high-grade lymphomas, FDG-PET/CT is the standard imaging

procedure in primary diagnosis and follow-up (194,195). Because chemotherapy is the first-line therapy and RT plays a minor role, only few clinical data are available regarding the impact of PET/CT in target volume delineation. However, two studies in 2003 and 2004 with a total of 41 patients could show substantial changes of target volumes when incorporating the PET information into the treatment planning process (150,196). More recent studies have confirmed the marked impact of PET/CT in the RT planning of Hodgkin lymphoma (197,198). Figure 5 shows the GTV delineated on the PET/CT scan of a patient with Stage IIA Hodgkin lymphoma, whereas PET revealed an additional FDG positive paratracheal lymph node that was missed on CT.

#### *Breast Cancer*

Despite excellent diagnostic specificity (>95%) for both primary tumor and axillary lymph node involvement, conventional whole-body PET and PET/CT provide only moderate sensitivity (40–85%) in invasive ductal breast cancer (199–204). Mavi et al (205) showed that a second, delayed scan at 120 minutes could markedly increase the sensitivity. Heusner et al (206) evaluated a specially designed acquisition protocol using the prone position and a positioning aid in 40 patients with suspected cancer recurrence. The authors report better delineation of potential infiltration of the adjacent thoracic wall and skin, but no significant benefit with respect to axillary staging. The same group assessed this protocol in comparison to MRI, ultrasound, and clinical investigation for primary tumor, local, and distant metastases (207). They concluded that whole-body FDG-PET/CT mammography could be used for staging breast cancer in a single session because the diagnostic accuracy for primary tumors is similar to MRI, whereas the detection rate of distant metastases was 100% compared to 70% when using a multimodality approach correlating x-ray mammography findings with breast ultrasound and MRI complemented by sentinel lymph

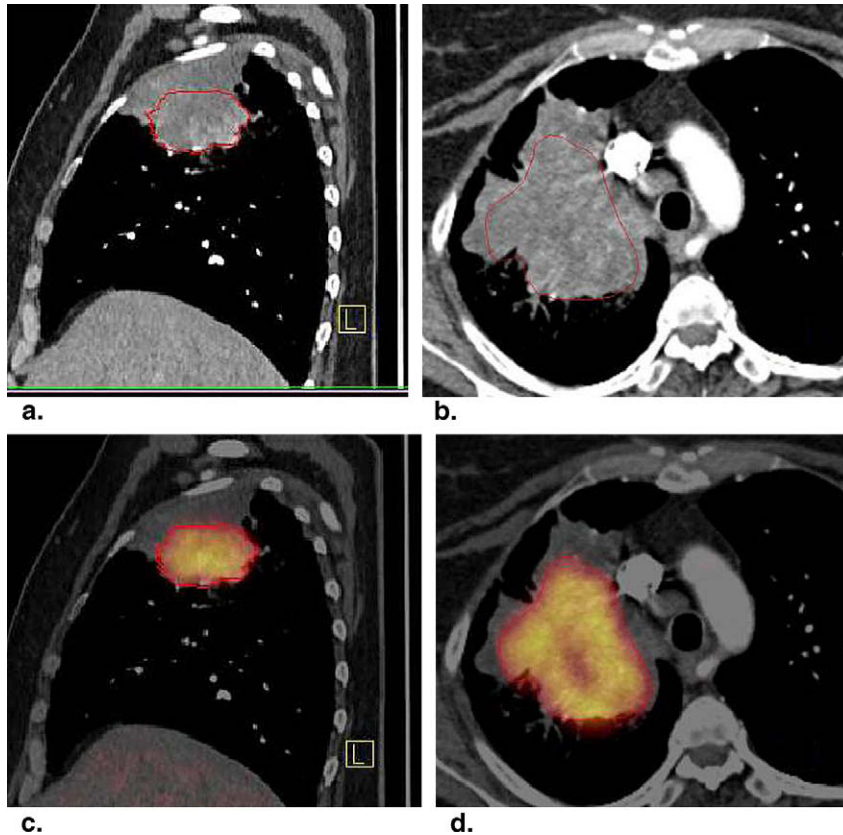


**Figure 5.** Sagittal and axial positron emission tomography/computed tomography (PET/CT) images of a patient with non-small-cell lung cancer of the right upper lobe. PET/CT allowed excluding associated atelectasis that was impossible using a diagnostic quality CT alone.

node biopsy, chest radiography, axillary and abdominal ultrasound, and bone scintigraphy. The overall change of treatment strategy for the patients included in this study was 12.5%. However, FDG-PET currently has no role in lobular carcinoma and carcinoma in situ because of the low tracer uptake. Based on these facts, few studies address the issue of FDG-PET based target volume delineation in breast cancer. Dizendorf et al (150) reported additional metastatic lymph nodes in 14% of the patients ( $n = 18$ ), leading to a modification of the target volume in 11% of the patients. Moreover, a recent feasibility study on 13 patients showed a marked impact of FDG-PET on dose distribution when including metabolic data into RT planning of breast cancer (208).

An evolving area for breast cancer is the introduction of dedicated breast PET scanners allowing to perform positron emission mammography examinations using optimized detector designs achieving higher spatial resolution and improved sensitivity (81,82,209–212). First clinical studies comparing positron emission mammography with conventional mammography reported 80% sensitivity, 100%

specificity, and 86% accuracy (213) and demonstrated a satisfying sensitivity for malignancy (86%) with a high positive predictive value (90%) (214). In terms of quantification of tracer uptake, a recent study using rotating high-resolution LYSO detectors with a reconstructed field-of-view of  $15 \times 15 \times 15 \text{ cm}^3$  reported promising results indicating the feasibility to use the device for early assessment of cancer treatment (215).

The integration of these novel technologies into the RT treatment planning process might be of great interest. However, many shortcomings need to be addressed beforehand, such as the complexity of non-rigid image registration with a larger field-of-view RT planning CT scan that would be required for dosimetry calculations (216). This is probably the main issue limiting the role of dedicated breast PET systems for GTV delineation in RT. Nevertheless, novel combined breast PET/CT scanners under development (eg, the system being designed by Boone et al at the University of California Davis) following the successful design of dedicated breast CT (217) and small-bore preclinical PET/CT (218) might play an emerging role in the future.

### Other Tumors

For a variety of other tumors, FDG-PET/CT–based target volume delineation plays no (or not yet) role in target volume delineation because of their low FDG avidity (eg, prostate cancer, renal cell carcinoma, neuroendocrine tumors), low tumor to background contrast (brain tumors), or because RT plays no major role in their treatment (malignant melanoma, bone and soft-tissue tumors, differentiated thyroid carcinoma). However, for some of them (eg, brain tumors, prostate cancer), other new and promising PET tracers are available for staging that can potentially be applied in target volume delineation for radiation therapy treatment planning. Those probes that have already been used are discussed in the following section.

### Novel Promising Probes beyond FDG for of PET-guided Target Volume Delineation

Besides FDG, many other more or less tumor-specific PET tracers have been introduced during the last few years (112,113). The most important are markers of tumor proliferation (eg,  $^{18}\text{F}$ -fluorothymidine), amino acid metabolism ( $^{11}\text{C}$ -methionine,  $^{11}\text{C}$ -tyrosine, and  $^{18}\text{F}$ -fluoro-ethyl-tyrosine), and hypoxia ( $^{18}\text{F}$ -fluoromisonidazole,  $^{18}\text{F}$ -fluoroazomycin-arabinofuranoside,  $^{64}\text{Cu}$ -ATSM, and  $^{18}\text{F}$ -EF5), which have already shown their importance in target volume delineation or patient management in RT (219,220) as discussed in the subsequent paragraphs.

In addition, new tracers have been developed that specifically bind to certain intra or extracellular compounds of various tumors, such as  $^{18}\text{F}$ -DOPA (metabolism of amine precursor uptake and decarboxylase tumors),  $^{68}\text{Ga}$ -labeled peptides (neuroendocrine tumors),  $^{11}\text{C}$ -acetate or  $^{11}\text{C}$ -choline, and  $^{18}\text{F}$ -choline (cell membrane and fatty acid metabolism). These tracers actually encounter a growing use in diagnosis, treatment planning, and control in many tumor entities. This section will mainly discuss the tracers with already proven relevance in patients undergoing RT. Table 2 summarizes current applications of non-FDG PET tracers for target volume delineation in RT treatment planning.

### Markers of Tumor Hypoxia

Experiments with tumor cell lines or tumor-bearing rodents have shown that tumor hypoxia reduces the response to RT (221–223). In addition, it is related to lower survival probability and higher risk of tumor recurrence (224,225). Therefore, radiation dose escalation in hypoxic tumor areas is deemed to increase treatment response and decrease local tumor recurrence. Now, mainly  $^{18}\text{F}$ -fluoromisonidazole and  $^{18}\text{F}$ -fluoroazomycin-arabinofuranoside, two chemically similar radiotracers, are used for hypoxia imaging. Wide experience was gained in head-and-neck tumors, where hypoxia imaging was shown to be useful for target volume delineation

(mostly in combination with FDG) in IMRT (19,116,226,227). However, not only head-and-neck tumors have been addressed as other studies reported on the usefulness of hypoxia imaging for other localizations such as lung, kidney, brain, and soft-tissue sarcomas (115,228–230). Moreover, hypoxia tracers have shown their potential to expose dynamic changes of reoxygenation during RT, which may have important implications in predicting treatment outcome (6,137,225,231). A new promising tracer is the lipophilic  $^{60}\text{Cu}$ -ATSM, which is less susceptible to reduction in the presence of oxygen and is thus rapidly washed out of normoxic tissue. The first studies assessed the correlation between hypoxic tissue and histology using autoradiography in a tumor-bearing mouse model (223). The prediction of treatment response in cervical cancer was one of the targeted applications (231).  $^{18}\text{F}$ -EF5 is another promising agent (232,233) that proved to be useful for noninvasive clinical assessment of hypoxia in brain tumors (234).

### Amino Acids

Several tumors present an increase of amino acid metabolism, which can be targeted by PET. Relevant experience worldwide was achieved for the following three tracers:  $^{11}\text{C}$ -MET,  $^{11}\text{C}$ -tyrosine, and  $^{18}\text{F}$ -fluoro-ethyl-tyrosine. Whereas the short half-life (~20 minutes) limits the use of  $^{11}\text{C}$ -labeled tracers to centers equipped with a cyclotron and tracer production facility close to the PET scanner,  $^{18}\text{F}$ -fluoro-ethyl-tyrosine is available for more widespread use. Up to now, these tracers are mainly used in brain tumor imaging (Table 2). First, they were applied to differentiate between scar and viable tissue in treated brain tumors since CT, MRI, or FDG-PET had high rates of equivocal or false positive findings. In 1997, Reinhardt et al (235) showed the usefulness and high specificity of  $^{14}\text{C}$ -methionine for viable tumor cells in a rat model. Later on, PET imaging using amino acid tracers showed their superiority compared to conventional MRI in diagnosis of tumor recurrence which resulted in significant change in patient management (236–240). Recently, these tracers were successfully used in radiosurgery or target volume delineation for primary or recurrent brain tumors, such as pituitary adenomas, meningiomas, gliomas, and glioblastomas. More importantly, substantial differences in terms of gross tumor delineation were reported when compared to CT- or MRI-based treatment planning (Figure 6) (148,236,241–250). Semiautomated target volume delineation algorithms have been successfully applied using these “positive” markers, which have an important advantage compared to FDG, namely that there is no nonspecific uptake in inflammatory reactions or macrophages (242,249).

### Cell Membranes/Fatty Acid Metabolism

$^{11}\text{C}$ -choline and  $^{18}\text{F}$ -fluoro-choline are supposed to undergo two metabolic pathways in cancer cells with high lipid turnover, such as prostate cancer. On the one hand, they are

Table 2

## Summary of Recent Contributions assessing the Impact of non-FDG PET Tracers for Target Volume Definition in Radiotherapy

Target	Tracer	Localization	Reference	n	Reference Method(s)	Results	Complementary Findings
Hypoxia	<sup>18</sup> F-MISO	Head and neck	(226)	10	FDG PET/CT, CT, MRI	Dose escalation to hypoxic tissue feasible in all cases (84–105 Gy) without exceeding normal tissue tolerance	Various levels of hypoxia demonstrated by heterogeneous <sup>18</sup> F-MISO distribution
	<sup>18</sup> F-FAZA	Head and neck	(116)	18	CT	Median GTV/FAZA represented 10.8% (0.7–52%) of the GTV/CT in the primary and 8.3% (2.2–51.3%) in the lymph nodes.	No significant correlation between GTV/FAZA and GTV/CT for the primary, significant correlation for the lymph nodes. Different patterns of hypoxia influenced dose painting.
	<sup>60</sup> Cu-ATSM	Cervical cancer	(334)	14	FDG PET, clinical follow-up	ATSM uptake significant predictor of progression free and overall survival	Frequency of locoregional nodal metastases significantly higher in hypoxic tumors; FDG uptake did not correlate with tumor hypoxia
Amino acid metabolism	<sup>11</sup> C-Methionine	Meningioma	(241)	32	CT, MRI	Methionine PET beneficial in 29/32 patients (91%) due to identification of small tumor portions not identified by CT or MRI. Mean GTV enlargement due to PET: 9.4 ± 10.7%	
		Meningioma	(148)	10	CT, MRI	Significant decrease of interobserver variability of GTV when adding the PET information ( $r = 0.855 \geq 0.988$ )	PET information helpful in GTV delineation in sinus cavernosus, orbit and skull base areas
	<sup>18</sup> F-FET	Malignant glioma	(240)	45	MRI	FET PET sensitivity 100%, specificity 92.9%; MRI sensitivity 93.5%, specificity 50%	Concordance between FET PET and MRI in 37 cases, discordance in 8 cases ( $P < .01$ )
		Malignant glioma	(335)	24	Pathology ( $n = 9$ ); clinical follow-up	Time course and pattern of serial FET PET acquisitions correlate well with success of intracavitary radioimmunotherapy	Threshold of 2.4 (tumor/background ratio) allows for discrimination between recurrence and inflammation (sensitivity 88%, specificity 100%)
	<sup>18</sup> F-FET	Malignant glioma	(249)	18	PET, MRI	The majority of GTVs defined on various PET-based segmentation techniques were usually smaller than GTV <sub>MRI</sub> (67% of cases)	PET detected frequently tumours that are not visible on MRI and added substantially tumour extension outside the GTV <sub>MRI</sub> in 6 patients (33% of cases)

**Table 2**  
(Continued)

Target	Tracer	Localization	Reference	n	Reference Method(s)	Results	Complementary Findings
Cell membranes/ fatty acid metabolism	<sup>18</sup> F-Fluorocholine	Prostate cancer	(257)	10	CT	Comparable results for target volumes derived from CT and PET. Optimal concordance for lateral and craniocaudal dimensions was achieved when using a signal threshold of $23.0 \pm 2.6\%$ , for anterior-posterior dimensions when applying a threshold of $49.5 \pm 4.6\%$	3-dimensional conformal treatment planning on Fluorocholine PET and CT alone delivered comparable doses to the rectal wall
Somatostatin receptors	<sup>68</sup> Ga-DOTA-TOC	Meningioma	(262)	26	CT, MRI	Significant modification of PTV based on DOTA-TOC PET in 19/26 patients (73%). Compared to CT PTVs alone, trimodal outlined PTVs decreased in 9/26 patients (35%) and increased in 10/26 patients (38%)	DOTA-TOC PET delivered additional information on tumor extension in all patients. In one patient, only DOTA-TOC PET was able to detect the lesion

ATSM, diacetyl-bis(N4-methylthiosemicarbazone); PET, positron emission tomography; CT, computed tomography; FDG, fluorodeoxyglucose; GTV, gross tumor volume; MRI, magnetic resonance imaging.

converted into phospholipids and included into the cell membrane, whereas on the other hand they are used in the energy metabolism undergoing beta-oxidation. Both lead to “metabolic” trapping and accumulation in cancer cells. Most experiences using these tracers are available for prostate cancer where their value was demonstrated for the detection of tumor recurrence (251–256). However, the sensitivity of the two probes seems to differ with respect to PSA level. More recently, first studies with promising results on the application of these tracers for target volume delineation in RT treatment planning of recurrent prostate cancer have been published (219,257–259). Figure 7 illustrates an <sup>18</sup>F-choline PET/CT study of a patient with recurrent tumor in the left posterior lobe that was confirmed by bilateral endorectal biopsy of the prostate. The GTV delineated for partial reirradiation of the prostate is also shown.

#### *Proliferation Markers*

Different probes belonging to this category of tracers are available. However, <sup>18</sup>F-fluorothymidine, a radioactive derivative of the nucleoside thymidine, is more widely used to determine tumor proliferation owing to its long half-life

(120). However, studies describing its use in target volume delineation have been lacking. The only results published so far address the issues of therapy control (260) and assessment of cancer recurrence (235) in a preclinical setting.

#### *Tracers for Neuroendocrine Tumors*

For targeting neuroendocrine tumors, two physiological principles are applied. Because many of them overexpress somatostatin receptors, positron-emitting labeled somatostatin analogues such as <sup>68</sup>Ga-DOTA-TOC have been developed. A recent study has shown the excellent sensitivity and specificity of this tracer (261). Another important advantage of <sup>68</sup>Ga-labeled tracers is that the radioisotope is eluted from a <sup>68</sup>Ge/<sup>68</sup>Ga generator and as such, an onsite cyclotron is not required for their production. However, these tracers may not cover all neuroendocrine tumors. Knowing that some of them belong to the amine precursor uptake and decarboxylase cell system, markers of the amine precursors such as <sup>18</sup>F-FDOPA can be applied for staging and therapy planning in these tumors (123). Despite their success in diagnosis and staging of recurrent neuroendocrine tumors, up to now, there is a lack of publications reporting on their

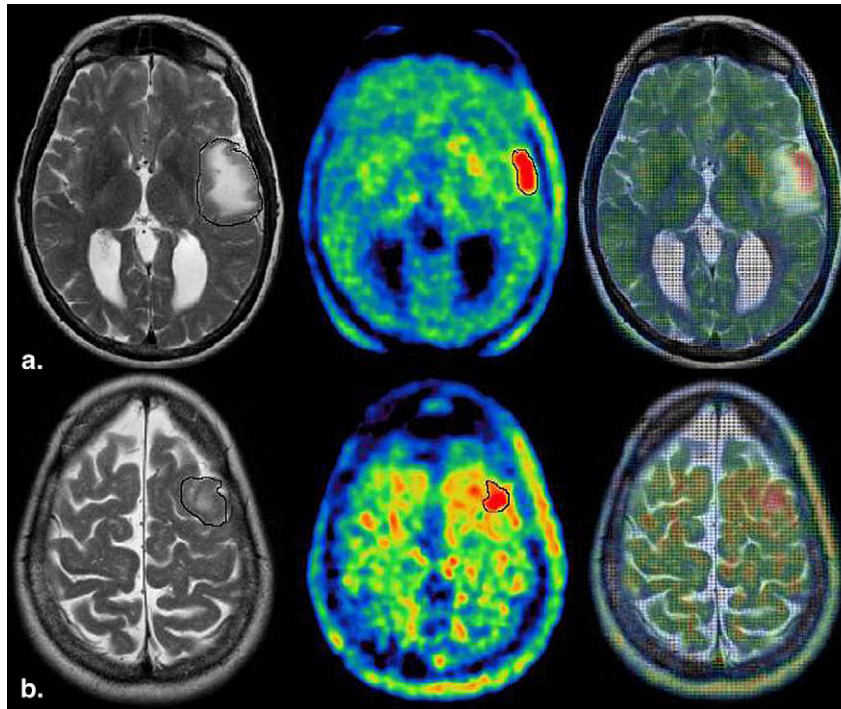


**Figure 6.** Example of a patient with a glioblastoma (World Health Organization IV) in the left temporal and frontal areas. The contrast enhanced T2-weighted magnetic resonance images and the  $^{18}\text{F}$ -fluoro-ethyl-tyrosine positron emission tomography show substantially different gross tumor volume extension on the two modalities (*black color*).

usefulness in RT treatment planning. The only published study on  $^{68}\text{Ga}$ -DOTA-TOC reported a substantial impact on target volume delineation in intracranial meningiomas when compared to CT and MRI (262).

### PET/CT-GUIDED DELINEATION OF TARGET VOLUMES

Historically, GTVs were defined on high resolution anatomical images despite the limitations of these techniques (263–268). CT can provide useful anatomical information and the electronic density required for dosimetry calculations for RT treatment planning. However, it has poor soft-tissue contrast that might be insufficient for target and critical organ delineation. MRI provides higher image quality and better soft-tissue contrast compared to CT. Many investigators reported significant differences in terms of target volume delineation when using MRI compared to CT (269,270). It has been argued that coregistered CT/MRI data can be used with confidence for accurate delineation of target volumes and critical organs (using MRI) and dose computation (using CT). For some applications (eg, prostate), MRI can even be used for both delineation and dosimetry calculations thus

allowing to improve patient throughput, reduce cost and radiation exposure to the patient (271,272).

Owing to the limitations discussed previously and after the widespread clinical adoption of hybrid PET/CT scanners, PET-based delineation of target volumes appeared as an attractive alternative for RT treatment planning (13,136,138,160,174,273–278). One of the most difficult issues facing PET-based RT treatment planning is the accurate delineation of target regions from typical noisy functional images (21). The major problems encountered in functional volume quantitation are image segmentation and imperfect system response function. Image segmentation is defined as the process of classifying the voxels of an image into a set of distinct classes. The difficulty in image segmentation is compounded by the low spatial resolution and high-noise characteristics of PET images. Medical image segmentation has been identified as the key problem of medical image analysis and remains a popular and challenging area of research (279). Despite the difficulties and known limitations, several image segmentation approaches have been proposed and used in clinical setting including thresholding, region growing, classifiers, clustering, edge detection, Markov random field models, artificial neural networks, deformable models, atlas-guided, and many other approaches (141,167,280). A detailed description of the

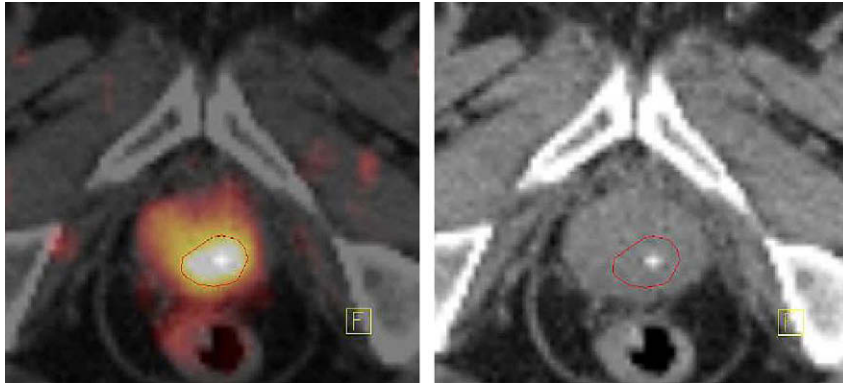


**Figure 7.** Patient with biochemically recurrent prostate cancer 6 years after initial radiotherapy.  $^{18}\text{F}$ -choline positron emission tomography/computed tomography (PET/CT) showed a recurrent tumor in the left posterior lobe. This tumor was confirmed by bilateral endorectal biopsy of the prostate. The gross tumor volume delineated for partial reirradiation of the prostate by intensity-modulated radiotherapy is shown (red color).

various approaches proposed so far is beyond the scope of this review and is discussed elsewhere (13). Here we briefly discuss some important considerations and limitations of widely used techniques.

Medical image segmentation remains an unsolved problem that has captured the imagination of image analysis scientists over the past three decades. Manual segmentation methods available on most commercial software packages to identify lesion boundaries and to quantify GTVs in terms of standardized uptake value are very laborious and tedious. They discourage physicians from taking advantage of the inherently quantitative data and compel them to use qualitative means in their diagnosis, therapy planning, and assessment of patient response to therapy. Semi- or fully automated segmentation methods enable physicians to easily extract maximum and mean standardized uptake value estimates from a lesion volume. This also allows the physician to track changes in lesion size and uptake after radiochemotherapy. At present, various methods are used in practice to delineate PET-based target volumes (158,167,177,178,249,281–295).

Manual delineation of target volumes using different window level settings and look up tables is the most common and widely used technique in the clinic. However, the method is highly operator-dependent and is subject to high variability between operators (161,177). Rather large intraobserver variability was reported for many localizations (155,250,296,297). In this respect, semi- or fully-automated delineation techniques might offer several advantages over manual techniques by reducing operator error/subjectivity, thereby improving reproducibility.

One major concern is that radiation oncologists had limited exposure to hybrid technologies and as such, they are not trained enough to read PET/CT scans and delineate auto-

mously the GTVs on PET images. A joint effort between experienced nuclear medicine physicians and radiation oncologists is therefore a prerequisite to fully exploit the potential of PET/CT-guided RT. Cross-training requirements and guidelines regarding the qualifications and training requirements of the physicians who interpret the images have been recently debated both in the United States (298) and in Europe (299). Similar discussions should, in our opinion, take place between nuclear medicine and radiation oncology professional societies to establish a common ground in the near future.

As discussed earlier, one of the challenges faced by vendors is to provide commercial platforms that can easily handle multimodality images from any DICOM-compatible imaging modality including hybrid PET/CT and incorporate this information with minimum effort into the RT treatment planning software. In essence, all vendors claim full DICOM compatibility, however, in real life, such statements cannot be taken as granted and need to be checked carefully by the end users. In our experience, all vendors allow to export to picture archiving and communication systems and incorporate PET/CT images in a clinical RT setting using the DICOM standard. However, the transfer of RT objects in DICOM\_RT format between various commercial platforms is more obscure and might effectively hinder research carried out in the field. In the authors' institution, a commercial PET/CT scanner with the associated multimodality workplace virtual simulation software (Siemens Medical Solutions) is used for delineation of GTV. We had to write software that converts the DICOM\_RT objects generated by the Siemens software in a format that is readable by the ACQSIM platform (Philips Medical Systems). Moreover, we are using extensively *RT\_Image*, an open-source software developed to facilitate the integration of PET/CT imaging in RT treatment planning (300) in our research

studies (249). We realized that the DICOM\_RT objects generated by the Siemens software can be read by this software; however, those generated by *RT\_Image* cannot be read by the Siemens virtual simulation software package owing to some incompatibility in DICOM tag information present in the file. Therefore, the lack of cooperation between the vendors may seriously hamper potential collaborative research projects owing to practical difficulties in incorporating the PET information in existing clinical RT settings.

### Validation and Comparison of Techniques

Despite the remarkable progress that image segmentation has made during the last few years, performance validation in a clinical setting remains the most challenging issue (301). There are basically three different strategies allowing the assessment of the accuracy of PET image segmentation techniques. This includes simulated or experimental phantom studies in which the ground truth (tumor volume) is known a priori, the comparison with correlated anatomical GTVs defined on CT or MRI, and the comparison of tumor volumes delineated on PET with actual tumor volumes measured on the macroscopic specimen derived from histology, in case a PET scan was undertaken before surgery. The shortcomings of experimental phantom studies where simple lesions simulating tumors' shapes and contrast are introduced within the phantom are well established. More accurate simulation techniques combining Monte Carlo and clinical data are now becoming available and will certainly allow comprehensive assessment of segmentation algorithms (27,302). On the other hand, when using clinical data where the ground truth is not known a priori, it is generally unacceptable to use an imaging modality as gold standard against which results from another imaging modality are compared. Only very few studies reported on the use of surgical specimen for validation of PET-based GTV delineation techniques (142,155,165,166,179,303–305). The only studies where the 3D macroscopic specimen (in contrast to lesion size defined on one to three major axes) was available clearly demonstrated the superiority of PET compared to other structural modalities for head-and-neck cancer (142,165).

A limited number of studies reported the comparative evaluation of different PET image segmentation techniques (178,249,284,306,307). The main difference between the image segmentation methods is the underlying empirical derivation or mathematical model used to differentiate between the tumor and background. Most comparative assessment studies seem to suggest that the differences in the estimated volumes did have a significant impact on the GTV. It has been difficult to establish the superiority of one method over another. Thus, we can argue that at present the important thing is to use the most reliable technique available to the

users, although ultimately it may become clear which method is best for a particular application.

### CHALLENGES AND FUTURE DIRECTIONS

Despite the remarkable progress achieved, as can be witnessed by the enormous number of publications in the field, many challenging issues still remain to be solved through research. There is no shortage of challenges and opportunities for molecular imaging-guided RT treatment planning now. Several PET segmentation algorithms have been developed so far with limited success. Tumor heterogeneity and stability of tracer uptake is one of the challenges facing automated delineation of GTVs (13,308).

PET/CT is at present mainly used for whole-body oncological studies, an application embracing the mainstream of reimbursable indications for PET/CT in the United States and many other countries. Reimbursement issues are mainly driven by prospective multicenter clinical trials that reveal enhancements in health outcomes conveyed by PET/CT as an imaging modality for a given indication: in this case, RT treatment planning. It is expected that ongoing research studies will undoubtedly allow to expand coverage for PET/CT scans by following the same trend as for other indications.

Respiratory motion is another challenging issue that has been addressed in many different ways. The most successful approaches attempt to overcome the limitations of the traditional approach, which allows obtaining individually reconstructed noisy images through respiratory gating by incorporating motion estimation and correction within the image reconstruction process to obtain images of enhanced quality (38,309–311). Image-based motion correction strategies look promising and deserve particular attention. It is a matter of public evidence that active research in the field has emerged from the recent 2008 IEEE Medical Imaging Conference in Dresden (312–316), recognized as the most production conference in medical imaging technology. Despite the much worthwhile research carried out in this direction, the field clearly deserves further research and development efforts (317). Overall, we believe that the best strategies for motion correction use increasingly sophisticated software to make use of existing advanced hardware. In this sense, the field is open to future novel ideas (hardware and especially software) aimed at improving motion detection, characterization, and compensation (318).

### REFERENCES

1. Cherry SR. In vivo molecular and genomic imaging: new challenges for imaging physics. *Phys Med Biol* 2004; 49:R13–R48.
2. Zaidi H, Alavi A. Current trends in PET and combined (PET/CT and PET/MR) systems design. *PET Clin* 2007; 2:109–123.
3. von Schulthess GK, Steinert HC, Hany TF. Integrated PET/CT: current applications and future directions. *Radiology* 2006; 238:405–422.

4. Juweid ME, Cheson BD. Positron-emission tomography and assessment of cancer therapy. *N Engl J Med* 2006; 354:496–507.
5. Blodgett TM, Meltzer CC, Townsend DW. PET/CT: form and function. *Radiology* 2007; 242:360–385.
6. Czernin J, Allen-Auerbach M, Schelbert HR. Improvements in cancer staging with PET/CT: literature-based evidence as of september 2006. *J Nucl Med* 2007; 48:78S–88S.
7. Townsend DW. Positron emission tomography/computed tomography. *Semin Nucl Med* 2008; 38:152–166.
8. Hasegawa B, Zaidi H. Dual-modality imaging: more than the sum of its components. In: Zaidi H, ed. *Quantitative analysis in nuclear medicine imaging*. New York: Springer, 2006; 35–81.
9. Goerres GW, von Schultheiss GK, Steinert HC. Why most PET of lung and head-and-neck cancer will be PET/CT. *J Nucl Med* 2004; 45:66S–71S.
10. Zaidi H, Montandon M-L, Alavi A. Advances in attenuation correction techniques in PET. *PET Clin* 2007; 2:191–217.
11. Zaidi H, Montandon M-L. Scatter compensation techniques in PET. *PET Clin* 2007; 2:219–234.
12. Soret M, Bacharach SL, Buvat I. Partial-volume effect in PET tumor imaging. *J Nucl Med* 2007; 48:932–945.
13. Zaidi H, El Naqa I. PET-guided delineation of radiation therapy treatment volumes: a review of image segmentation techniques. *Med Image Anal*. In press.
14. Bortfeld T. IMRT: a review and preview. *Phys Med Biol* 2006; 51: R363–R379.
15. Ling CC, Yorke E, Fuks Z. From IMRT to IGRT: frontierland or neverland? *Radiother Oncol* 2006; 78:119–122.
16. Bentzen SM. Theragnostic imaging for radiation oncology: dose-painting by numbers. *Lancet Oncol* 2005; 6:112–117.
17. Bentzen SM. Dose painting and theragnostic imaging: towards the prescription, planning and delivery of biologically targeted dose distributions in external beam radiation oncology. *Cancer Treat Res* 2008; 139:41–62.
18. Chapman JD, Bradley JD, Eary JF, et al. Molecular (functional) imaging for radiotherapy applications: an RTOG symposium. *Int J Radiat Oncol Biol Phys* 2003; 55:294–301.
19. Grosu AL, Wiedenmann N, Molls M. Biological imaging in radiation oncology. *Z Med Phys* 2005; 15:141–145.
20. Messa C, Di Muzio N, Picchio M, et al. PET/CT and radiotherapy. *Q J Nucl Med Mol Imaging* 2006; 50:4–14.
21. Gregoire V, Haustermans K, Geets X, et al. PET-based treatment planning in radiotherapy: a new standard? *J Nucl Med* 2007; 48: 68S–77S.
22. Lecchi M, Fossati P, Elisei F, et al. Current concepts on imaging in radiotherapy. *Eur J Nucl Med Mol Imaging* 2008; 35:821–837.
23. Mah D, Chen CC. Image guidance in radiation oncology treatment planning: the role of imaging technologies on the planning process. *Semin Nucl Med* 2008; 38:114–118.
24. Xing L, Wessels B. The value of PET/CT is being over-sold as a clinical tool in radiation oncology. *Med Phys* 2005; 32:1457–1459.
25. Pan T, Chen L, Orton CG. PET/CT will become standard practice for radiotherapy simulation and planning. *Med Phys* 2008; 35:3825–3827.
26. Ollers M, Bosmans G, van Baardwijk A, et al. The integration of PET-CT scans from different hospitals into radiotherapy treatment planning. *Radiother Oncol* 2008; 87:142–146.
27. Aristophanous M, Penney BC, Pelizzari CA. The development and testing of a digital PET phantom for the evaluation of tumor volume segmentation techniques. *Med Phys* 2008; 35:3331–3342.
28. Bernier J, Hall EJ, Giaccia A. Radiation oncology: a century of achievements. *Nat Rev Cancer* 2004; 4:737–747.
29. Webb S, Evans PM. Innovative techniques in radiation therapy: editorial, overview, and crystal ball gaze to the future. *Semin Radiat Oncol* 2006; 16:193–198.
30. Perez CA, Purdy JA, Harms W, et al. Three-dimensional treatment planning and conformal radiation therapy: preliminary evaluation. *Radiother Oncol* 1995; 36:32–43.
31. Stroom JC, Korevaar GA, Koper PC, et al. Multiple two-dimensional versus three-dimensional PTV definition in treatment planning for conformal radiotherapy. *Radiother Oncol* 1998; 47:297–302.
32. Dobbs HJ, Parker RP. The respective roles of the simulator and computed tomography in radiotherapy planning: a review. *Clin Radiol* 1984; 35:433–439.
33. Lu R, Radke RJ, Happersett L, et al. Reduced-order parameter optimization for simplifying prostate IMRT planning. *Phys Med Biol* 2007; 52:849–870.
34. Chang BK, Timmerman RD. Stereotactic body radiation therapy: a comprehensive review. *Am J Clin Oncol* 2007; 30:637–644.
35. Pan T, Lee TY, Rietzel E, et al. 4D-CT imaging of a volume influenced by respiratory motion on multi-slice CT. *Med Phys* 2004; 31:333–340.
36. Rietzel E, Pan T, Chen GT. Four-dimensional computed tomography: image formation and clinical protocol. *Med Phys* 2005; 32:874–889.
37. Keall P, Vedam S, George R, et al. The clinical implementation of respiratory-gated intensity-modulated radiotherapy. *Med Dosim* 2006; 31:152–162.
38. Li XA, Keall PJ. Respiratory gating for radiation therapy is not ready for prime time. *Med Phys* 2007; 34:867–870.
39. Li G, Citrin D, Camphausen K, et al. Advances in 4D medical imaging and 4D radiation therapy. *Technol Cancer Res Treat* 2008; 7:67–82.
40. Erdi YE, Nehmeh SA, Pan T, et al. The CT motion quantification of lung lesions and its impact on PET-measured SUVs. *J Nucl Med* 2004; 45: 1287–1292.
41. Nehmeh SA, Erdi YE, Pan T, et al. Four-dimensional (4D) PET/CT imaging of the thorax. *Med Phys* 2004; 31:3179–3186.
42. Nehmeh SA, Erdi YE, Pan T, Yorke E, et al. Quantitation of respiratory motion during 4D-PET/CT acquisition. *Med Phys* 2004; 31:1333–1338.
43. Lamare F, Ledesma Carbayo MJ, Cresson T, et al. List-mode-based reconstruction for respiratory motion correction in PET using non-rigid body transformations. *Phys Med Biol* 2007; 52:5187–5204.
44. Li T, Thorndyke B, Schreiber E, et al. Model-based image reconstruction for four-dimensional PET. *Med Phys* 2006; 33:1288–1298.
45. Nehmeh SA, Erdi YE. Respiratory motion in positron emission tomography/computed tomography: a review. *Semin Nucl Med* 2008; 38: 167–176.
46. Dawood M, Buther F, Jiang X, et al. Respiratory motion correction in 3-D PET data with advanced optical flow algorithms. *IEEE Trans Med Imaging* 2008; 27:1164–1175.
47. Papanthassiou D, Becker S, Amir R, et al. Respiratory motion artefact in the liver dome on FDG PET/CT: comparison of attenuation correction with CT and a caesium external source. *Eur J Nucl Med Mol Imaging* 2005; 32:1422–1428.
48. Osman MM, Cohade C, Nakamoto Y, et al. Clinically significant inaccurate localization of lesions with PET/CT: frequency in 300 patients. *J Nucl Med* 2003; 44:240–243.
49. Pan T, Mawlawi O, Nehmeh SA, et al. Attenuation correction of PET images with respiration-averaged CT images in PET/CT. *J Nucl Med* 2005; 46:1481–1487.
50. Xing L, Thorndyke B, Schreiber E, et al. Overview of image-guided radiation therapy. *Med Dosim* 2006; 31:91–112.
51. Shirato H, Shimizu S, Kitamura K, et al. Organ motion in image-guided radiotherapy: lessons from real-time tumor-tracking radiotherapy. *Int J Clin Oncol* 2007; 12:8–16.
52. Xing L, Siebers J, Keall P. Computational challenges for image-guided radiation therapy: framework and current research. *Semin Radiat Oncol* 2007; 7:245–257.
53. Fenwick JD, Tome WA, Soisson ET, et al. Tomotherapy and other innovative IMRT delivery systems. *Semin Radiat Oncol* 2006; 16: 199–208.
54. Mackie TR. History of tomotherapy. *Phys Med Biol* 2006; 51: R427–R453.
55. Otto K. Volumetric modulated arc therapy: IMRT in a single gantry arc. *Med Phys* 2008; 35:310–317.
56. Cozzi L, Dinshaw KA, Shrivastava SK, et al. A treatment planning study comparing volumetric arc modulation with RapidArc and fixed field IMRT for cervix uteri radiotherapy. *Radiother Oncol* 2008; 89:180–191.
57. Ling CC, Zhang P, Archambault Y, et al. Commissioning and quality assurance of RapidArc radiotherapy delivery system. *Int J Radiat Oncol Biol Phys* 2008; 72:575–581.
58. Brahme A. Recent advances in light ion radiation therapy. *Int J Radiat Oncol Biol Phys* 2004; 58:603–616.

59. Amaldi U. Future trends in cancer therapy with particle accelerators. *Z Med Phys* 2004; 14:7–16.
60. Brada M, Pijls-Johannesma M, De Ruyscher D. Proton therapy in clinical practice: current clinical evidence. *J Clin Oncol* 2007; 25: 965–970.
61. Jakel O, Karger CP, Debus J. The future of heavy ion radiotherapy. *Med Phys* 2008; 35:5653–5663.
62. Yoneoka Y, Tsumanuma I, Fukuda M, et al. Cranial base chordoma—long term outcome and review of the literature. *Acta Neurochir (Wien)* 2008; 150:773–778. discussion 778.
63. Pommier P, Liebsch NJ, Deschler DG, et al. Proton beam radiation therapy for skull base adenoid cystic carcinoma. *Arch Otolaryngol Head Neck Surg* 2006; 132:1242–1249.
64. Delaney TF, Liebsch NJ, Pedlow FX, et al. Phase II study of high-dose photon/proton radiotherapy in the management of spine sarcomas. *Int J Radiat Oncol Biol Phys*. In press.
65. Habrand JL, Schneider R, Alapetite C, et al. Proton therapy in pediatric skull base and cervical canal low-grade bone malignancies. *Int J Radiat Oncol Biol Phys* 2008; 71:672–675.
66. Rutz HP, Weber DC, Goitein G, et al. Postoperative spot-scanning proton radiation therapy for chordoma and chondrosarcoma in children and adolescents: initial experience at Paul Scherrer Institute. *Int J Radiat Oncol Biol Phys* 2008; 71:220–225.
67. Combs SE, Nikoghosyan A, Jaekel O, et al. Carbon ion radiotherapy for pediatric patients and young adults treated for tumors of the skull base. *Cancer* 2009; 115:1348–1355.
68. Bennett GW, Archambeau JO, Archambeau BE, et al. Visualization and transport of positron emission from proton activation in vivo. *Science* 1978; 200:1151–1153.
69. Pawelke J, Byars L, Enghardt W, et al. The investigation of different cameras for in-beam PET imaging. *Phys Med Biol* 1996; 41:279–296.
70. Crespo P, Shakirin G, Enghardt W. On the detector arrangement for in-beam PET for hadron therapy monitoring. *Phys Med Biol* 2006; 51: 2143–2163.
71. Attanasi F, Belcari N, Del Guerra A, et al. Comparison of two dedicated 'in beam' PET systems via simultaneous imaging of (12)C-induced beta(+)-activity. *Phys Med Biol* 2009; 54:N29–N35.
72. Nassalski A, Kapusta M, Batsch T, et al. Comparative study of scintillators for PET/CT detectors. *IEEE Trans Nucl Sci* 2007; 54:3–10.
73. Parodi K, Paganetti H, Cascio E, et al. PET/CT imaging for treatment verification after proton therapy: a study with plastic phantoms and metallic implants. *Med Phys* 2007; 34:419–435.
74. Kirkby C, Stanescu T, Rathée S, et al. Patient dosimetry for hybrid MRI-radiotherapy systems. *Med Phys* 2008; 35:1019–1027.
75. Hasegawa BH, Gingold EL, Reilly SM, et al. Description of a simultaneous emission-transmission CT system. *Proc SPIE* 1990; 1231:50–60.
76. Beyer T, Townsend D, Brun T, et al. A combined PET/CT scanner for clinical oncology. *J Nucl Med* 2000; 41:1369–1379.
77. Townsend D, Kinahan P, Beyer T. Attenuation correction for a combined 3D PET/CT scanner. *Phys Medica* 1996; 12(Suppl 1):43–48.
78. Klutz PG, Meltzer CC, Villemagne VL, et al. Combined PET/CT imaging in oncology. Impact on patient management. *Clin Positron Imaging* 2000; 3:223–230.
79. Muehlethner G, Karp JS. Positron emission tomography. *Phys Med Biol* 2006; 51:R117–R137.
80. Zaidi H. Recent developments and future trends in nuclear medicine instrumentation. *Z Med Phys* 2006; 16:5–17.
81. Thompson CJ. Instrumentation for positron emission mammography. *PET Clin* 2006; 1:33–38.
82. Weinberg IN. Applications for positron emission mammography. *Phys Med* 2006; 21(Suppl1):132–137.
83. Huber JS, Choong WS, Moses WW, et al. Initial results of a positron tomograph for prostate imaging. *IEEE Trans Nucl Sci* 2006; 53: 2653–2659.
84. Surti S, Kuhn A, Werner ME, et al. Performance of Philips Gemini TF PET/CT scanner with special consideration for its time-of-flight imaging capabilities. *J Nucl Med* 2007; 48:471–480.
85. Karp JS, Surti S, Daube-Witherspoon ME, et al. Benefit of time-of-flight in PET: experimental and clinical results. *J Nucl Med* 2008; 49:462–470.
86. Brenner DJ, Hall EJ. Computed tomography—an increasing source of radiation exposure. *N Engl J Med* 2007; 357:2277–2784.
87. Mori S, Endo M, Tsunoo T, et al. Physical performance evaluation of a 256-slice CT-scanner for four-dimensional imaging. *Med Phys* 2004; 31:1348–1356.
88. Klingebiel R, Siebert E, Diekmann S, et al. 4-D Imaging in cerebrovascular disorders by using 320-slice CT: feasibility and preliminary clinical experience. *Acad Radiol* 2009; 16:123–129.
89. Kalender WA. X-ray computed tomography. *Phys Med Biol* 2006; 51: R29–R43.
90. Boone JM. Multidetector CT: opportunities, challenges, and concerns associated with scanners with 64 or more detector rows. *Radiology* 2006; 241:334–337.
91. Steinert HC, von Schulthess GK. Initial clinical experience using a new integrated in-line PET/CT system. *Br J Radiol* 2002; 73:S36–S38.
92. Zaidi H. Is radionuclide transmission scanning obsolete for dual-modality PET/CT systems? *Eur J Nucl Med Mol Imaging* 2007; 34:815–818.
93. Alavi A, Mavi A, Basu S, Fischman A. Is PET-CT the only option? *Eur J Nuc Med Mol Imaging* 2007; 34:819–821.
94. Gambhir S, Czernin J, Schwimmer J, et al. A tabulated summary of the FDG PET literature. *J Nucl Med* 2001; 45:1S–93S.
95. Lardinois D, Weder W, Hany TF, et al. Staging of non-small-cell lung cancer with integrated positron-emission tomography and computed tomography. *N Engl J Med* 2003; 348:2500–2507.
96. Bar-Shalom R, Yefemov N, Guralnik L, et al. Clinical performance of PET/CT in evaluation of cancer: additional value for diagnostic imaging and patient management. *J Nucl Med* 2003; 44:1200–1209.
97. Cohade C, Wahl RL. Applications of positron emission tomography/computed tomography image fusion in clinical positron emission tomography—clinical use, interpretation, methods, diagnostic improvements. *Semin Nucl Med* 2003; 33:228–237.
98. Cherry SR. Multimodality in vivo imaging systems: twice the power or double the trouble? *Annu Rev Biomed Eng* 2006; 8:35–62.
99. Zaidi H, Mawlawi O. Simultaneous PET/MR will replace PET/CT as the molecular multimodality imaging platform of choice. *Med Phys* 2007; 34:1525–1528.
100. Pichler BJ, Wehrl HF, Kolb A, et al. Positron emission tomography/magnetic resonance imaging: the next generation of multimodality imaging? *Semin Nucl Med* 2008; 38:199–208.
101. Schlemmer HP, Pichler BJ, Schmand M, et al. Simultaneous MR/PET imaging of the human brain: feasibility study. *Radiology* 2008; 248: 1028–1035.
102. Zaidi H, Montandon M-L, Slosman DO. Magnetic resonance imaging-guided attenuation and scatter corrections in three-dimensional brain positron emission tomography. *Med Phys* 2003; 30:937–948.
103. Zaidi H. Is MRI-guided attenuation correction a viable option for dual-modality PET/MR imaging? *Radiology* 2007; 244:639–642.
104. Hofmann M, Steinke F, Scheel V, et al. MRI-based attenuation correction for PET/MRI: a novel approach combining pattern recognition and Atlas registration. *J Nucl Med* 2008; 49:1875–1883.
105. Gaa J, Rummeny EJ, Seemann MD. Whole-body imaging with PET/MRI. *Eur J Med Res* 2004; 30:309–312.
106. Seemann MD. Whole-body PET/MRI: the future in oncological imaging. *Technol Cancer Res Treat* 2005; 4:577–582.
107. Schlemmer HP, Pichler BJ, Krieg R, et al. An integrated MR/PET system: prospective applications. *Abdom Imaging*. In press.
108. Hicks RJ, Lau EW. PET/MRI: a different spin from under the rim. *Eur J Nucl Med Mol Imaging* 2009; 36:10–14.
109. Payne GS, Leach MO. Applications of magnetic resonance spectroscopy in radiotherapy treatment planning. *Br J Radiol* 2006; 79(Spec No 1):S16–S26.
110. Torigian DA, Huang SS, Houseni M, et al. Functional imaging of cancer with emphasis on molecular techniques. *CA Cancer J Clin* 2007; 57: 206–224.
111. Schoder H, Ong SC. Fundamentals of molecular imaging: rationale and applications with relevance for radiation oncology. *Semin Nucl Med* 2008; 38:119–128.
112. Kumar R, Dhanpathi H, Basu S, et al. Oncologic PET tracers beyond [(18)F]FDG and the novel quantitative approaches in PET imaging. *Q J Nucl Med Mol Imaging* 2008; 52:50–65.

113. Fowler JS, Ding YS, Volkow ND. Radiotracers for positron emission tomography imaging. *Semin Nucl Med* 2003; 33:14–27.
114. Weber WA, Figlin R. Monitoring cancer treatment with PET/CT: does it make a difference? *J Nucl Med* 2007; 48:36S–44S.
115. Evans SM, Fraker D, Hahn SM, et al. EF5 binding and clinical outcome in human soft tissue sarcomas. *Int J Radiat Oncol Biol Phys* 2006; 64: 922–927.
116. Grosu AL, Souvatzoglou M, Roper B, et al. Hypoxia imaging with FAZA-PET and theoretical considerations with regard to dose painting for individualization of radiotherapy in patients with head and neck cancer. *Int J Radiat Oncol Biol Phys* 2007; 69:541–551.
117. Wong TZ, Lacy JL, Petry NA, et al. PET of hypoxia and perfusion with  $^{62}\text{Cu}$ -ATSM and  $^{62}\text{Cu}$ -PTSM using a  $^{62}\text{Zn}/^{62}\text{Cu}$  generator. *AJR Am J Roentgenol* 2008; 190:427–432.
118. Nehmeh SA, Lee NY, Schroder H, et al. Reproducibility of intratumor distribution of (18F)-fluoromisonidazole in head and neck cancer. *Int J Radiat Oncol Biol Phys* 2008; 70:235–242.
119. Rajendran JG, Hendrickson KR, Spence AM, et al. Hypoxia imaging-directed radiation treatment planning. *Eur J Nucl Med Mol Imaging* 2006; 33(Suppl 1):44–53.
120. Mankoff D, Shields A, Krohn K. PET imaging of cellular proliferation. *Radiol Clin North Am* 2005; 43:153–167.
121. Fischman A. Role of [18F]-dopa-PET imaging in assessing movement disorders. *Radiol Clin North Am* 2005; 43:93–106.
122. Jager PL, Chirakal R, Marriott CJ, et al. 6-L-18F-Fluorodihydroxyphenylalanine PET in neuroendocrine tumors: Basic aspects and emerging clinical applications. *J Nucl Med* 2008; 49:573–586.
123. Nanni C, Fanti S, Rubello D. 18F-DOPA PET and PET/CT. *J Nucl Med* 2007; 48:1577–1579.
124. Belvisi L, Bernardi A, Colombo M, et al. Targeting integrins: insights into structure and activity of cyclic RGD pentapeptide mimics containing azabicycloalkane amino acids. *Bioorg Med Chem* 2006; 14:169–180.
125. Beer AJ, Grosu AL, Carlsen J, et al. [18F]Galacto-RGD positron emission tomography for imaging of  $\alpha_v\beta_3$  expression on the neovasculature in patients with squamous cell carcinoma of the head and neck. *Clin Cancer Res* 2007; 13:6610–6616.
126. Couturier O, Luxen A, Chatal JF, et al. Fluorinated tracers for imaging cancer with positron emission tomography. *Eur J Nucl Med Mol Imaging* 2004; 31:1182–1206.
127. Blankenberg F, Katsikis P, Tait J, et al. In vivo detection and imaging of phosphatidylserine expression during programmed cell death. *Proc Natl Acad Sci U S A* 1998; 95:6349–6354.
128. Rahn AN, Baum RP, Adamietz IA, et al. (Value of 18F fluorodeoxyglucose positron emission tomography in radiotherapy planning of head-neck tumors). *Strahlenther Onkol* 1998; 174:358–364.
129. Gross MW, Weber WA, Feldmann HJ, et al. The value of F-18-fluorodeoxyglucose PET for the 3-D radiation treatment planning of malignant gliomas. *Int J Radiat Oncol Biol Phys* 1998; 41:989–995.
130. Kiffer JD, Berlangieri SU, Scott AM, et al. The contribution of 18F-fluoro-2-deoxy-glucose positron emission tomographic imaging to radiotherapy planning in lung cancer. *Lung Cancer* 1998; 19:167–177.
131. Scarfone C, Jaszczak RJ, Gilland DR, et al. Quantitative pulmonary single photon emission computed tomography for radiotherapy applications. *Med Phys* 1999; 26:1579–1588.
132. Munley MT, Marks LB, Scarfone C, et al. Multimodality nuclear medicine imaging in three-dimensional radiation treatment planning for lung cancer: challenges and prospects. *Lung Cancer* 1999; 23:105–114.
133. Nestle U, Walter K, Schmidt S, et al. 18F-deoxyglucose positron emission tomography (FDG-PET) for the planning of radiotherapy in lung cancer: high impact in patients with atelectasis. *Int J Radiat Oncol Biol Phys* 1999; 44:593–597.
134. Vanuytsel LJ, Vansteenkiste JF, Stroobants SG, et al. The impact of 18F-fluoro-2-deoxy-glucose positron emission tomography (FDG-PET) lymph node staging on the radiation treatment volumes in patients with non-small cell lung cancer. *Radiother Oncol* 2000; 55:317–324.
135. Levivier M, Wikier D, Goldman S, et al. Integration of the metabolic data of positron emission tomography in the dosimetry planning of radio-surgery with the gamma knife: early experience with brain tumors. Technical note. *J Neurosurg* 2000; 93(Suppl 3):233–238.
136. Ling C, Humm J, Larson S, et al. Towards multidimensional radiotherapy (MD-CRT): biological imaging and biological conformality. *Int J Radiat Oncol Biol Phys* 2000; 47:551–560.
137. Scarfone C, Lavelly WC, Cmelak AJ, et al. Prospective feasibility trial of radiotherapy target definition for head and neck cancer using 3-dimensional PET and CT imaging. *J Nucl Med* 2004; 45:543–552.
138. Paulino AC, Thorstad WL, Fox T. Role of fusion in radiotherapy treatment planning. *Semin Nucl Med* 2003; 33:238–243.
139. Yap JT, Carney JP, Hall NC, Townsend DW. Image-guided cancer therapy using PET/CT. *Cancer J* 2004; 10:221–233.
140. Brunetti J, Caggiano A, Rosenbluth B, et al. Technical aspects of positron emission tomography/computed tomography fusion planning. *Semin Nucl Med* 2008; 38:129–136.
141. Greco C, Rosenzweig K, Cascini GL, et al. Current status of PET/CT for tumour volume definition in radiotherapy treatment planning for non-small cell lung cancer (NSCLC). *Lung Cancer* 2007; 57:125–134.
142. Stroom J, Blaauwgeers H, van Baardwijk A, et al. Feasibility of pathology-correlated lung imaging for accurate target definition of lung tumors. *Int J Radiat Oncol Biol Phys* 2007; 69:267–275.
143. Mah K, Caldwell CB, Ung YC, et al. The impact of (18)FDG-PET on target and critical organs in CT-based treatment planning of patients with poorly defined non-small-cell lung carcinoma: a prospective study. *Int J Radiat Oncol Biol Phys* 2002; 52:339–350.
144. Caldwell CB, Mah K, Skinner M, et al. Can PET provide the 3D extent of tumor motion for individualized internal target volumes? A phantom study of the limitations of CT and the promise of PET. *Int J Radiat Oncol Biol Phys* 2003; 55:1381–1393.
145. Bradley J, Thorstad WL, Mutic S, et al. Impact of FDG-PET on radiation therapy volume delineation in non-small-cell lung cancer. *Int J Radiat Oncol Biol Phys* 2004; 59:78–86.
146. Nestle U, Kremp S, Grosu AL. Practical integration of [18F]-FDG-PET and PET-CT in the planning of radiotherapy for non-small cell lung cancer (NSCLC): the technical basis, ICRU-target volumes, problems, perspectives. *Radiother Oncol* 2006; 81:209–225.
147. Levy RP. PET-CT: evolving role in 3-D radiation therapy. *Technol Cancer Res Treat* 2006; 5:101–107.
148. Grosu AL, Weber WA, Astner ST, et al.  $^{11}\text{C}$ -methionine PET improves the target volume delineation of meningiomas treated with stereotactic fractionated radiotherapy. *Int J Radiat Oncol Biol Phys* 2006; 66: 339–344.
149. Macapinlac HA. Clinical applications of positron emission tomography/computed tomography treatment planning. *Semin Nucl Med* 2008; 38: 137–140.
150. Dizendorf EV, Baumert BG, von Schulthess GK, et al. Impact of whole-body 18F-FDG PET on staging and managing patients for radiation therapy. *J Nucl Med* 2003; 44:24–29.
151. Czernin J, Phelps ME. Positron emission tomography scanning: current and future applications. *Annu Rev Med* 2002; 53:89–112.
152. Lammering G, De Haas D, De Ruyscher D, et al. First report on the use of a dedicated combined CT-PET simulator in rectal cancer patients [abstract]. *Radiother Oncol* 2004; ESTRO 23:S441.
153. Weder W, Schmid RA, Bruchhaus H, et al. C. Detection of extrathoracic metastases by positron emission tomography in lung cancer. *Ann Thorac Surg* 1998; 66:886–892; discussion 892–893.
154. Kaiff V, Hicks RJ, MacManus MP, et al. Clinical impact of (18)F fluorodeoxyglucose positron emission tomography in patients with non-small-cell lung cancer: a prospective study. *J Clin Oncol* 2001; 19: 111–118.
155. van Baardwijk A, Bosmans G, Boersma L, et al. PET-CT-based auto-contouring in non-small-cell lung cancer correlates with pathology and reduces interobserver variability in the delineation of the primary tumor and involved nodal volumes. *Int J Radiat Oncol Biol Phys* 2007; 68: 771–778.
156. Caldwell CB, Mah K, Ung YC, et al. Observer variation in contouring gross tumor volume in patients with poorly defined non-small-cell lung tumors on CT: the impact of 18FDG-hybrid PET fusion. *Int J Radiat Oncol Biol Phys* 2001; 51:923–931.
157. Fox JL, Rengan R, O'Meara W, et al. Does registration of PET and planning CT images decrease interobserver and intraobserver variation

- in delineating tumor volumes for non-small-cell lung cancer? *Int J Radiat Oncol Biol Phys* 2005; 62:70–75.
158. Ciernik IF, Dizendorf E, Baumert BG, et al. Radiation treatment planning with an integrated positron emission and computer tomography (PET/CT): a feasibility study. *Int J Radiat Oncol Biol Phys* 2003; 57:853–863.
  159. Deniaud-Alexandre E, Touboul E, Lerouge D, et al. Impact of computed tomography and 18F-deoxyglucose coincidence detection emission tomography image fusion for optimization of conformal radiotherapy in non-small-cell lung cancer. *Int J Radiat Oncol Biol Phys* 2005; 63:1432–1441.
  160. Ashamalla H, Rafla S, Parikh K, et al. The contribution of integrated PET/CT to the evolving definition of treatment volumes in radiation treatment planning in lung cancer. *Int J Radiat Oncol Biol Phys* 2005; 63:1016–1023.
  161. Hong R, Halama J, Bova D, et al. Correlation of PET standard uptake value and CT window-level thresholds for target delineation in CT-based radiation treatment planning. *Int J Radiat Oncol Biol Phys* 2007; 67:720–726.
  162. Paulino AC, Koshy M, Howell R, et al. Comparison of CT- and FDG-PET-defined gross tumor volume in intensity-modulated radiotherapy for head-and-neck cancer. *Int J Radiat Oncol Biol Phys* 2005; 61:1385–1392.
  163. Schwartz DL, Ford EC, Rajendran J, et al. FDG-PET/CT-guided intensity modulated head and neck radiotherapy: a pilot investigation. *Head Neck* 2005; 27:478–487.
  164. Geets X, Daisne JF, Tomsej M, et al. Impact of the type of imaging modality on target volumes delineation and dose distribution in pharyngo-laryngeal squamous cell carcinoma: comparison between pre- and per-treatment studies. *Radiother Oncol* 2006; 78:291–297.
  165. Daisne JF, Duprez T, Weynand B, et al. Tumor volume in pharyngolaryngeal squamous cell carcinoma: comparison at CT, MR imaging, and FDG PET and validation with surgical specimen. *Radiology* 2004; 233:93–100.
  166. Burri RJ, Rangaswamy B, Kostakoglu L, et al. Correlation of positron emission tomography standard uptake value and pathologic specimen size in cancer of the head and neck. *Int J Radiat Oncol Biol Phys* 2008; 71:682–628.
  167. van Baardwijk A, Baumert BG, Bosmans G, et al. The current status of FDG-PET in tumour volume definition in radiotherapy treatment planning. *Cancer Treat Rev* 2006; 32:245–260.
  168. Vernon MR, Maheshwari M, Schultz CJ, et al. Clinical outcomes of patients receiving integrated PET/CT-guided radiotherapy for head and neck carcinoma. *Int J Radiat Oncol Biol Phys* 2008; 70:678–684.
  169. Weng E, Tran L, Rege S, et al. Accuracy and clinical impact of mediastinal lymph node staging with FDG-PET imaging in potentially resectable lung cancer. *Am J Clin Oncol* 2000; 23:47–52.
  170. De Ruyscher D, Wanders S, Minken A, et al. Effects of radiotherapy planning with a dedicated combined PET-CT-simulator of patients with non-small cell lung cancer on dose limiting normal tissues and radiation dose-escalation: a planning study. *Radiother Oncol* 2005; 77:5–10.
  171. Messa C, Ceresoli GL, Rizzo G, et al. Feasibility of [18F]FDG-PET and coregistered CT on clinical target volume definition of advanced non-small cell lung cancer. *Q J Nucl Med Mol Imaging* 2005; 49:259–266.
  172. Luketich JD, Friedman DM, Meltzer CC, et al. The role of positron emission tomography in evaluating mediastinal lymph node metastases in non-small-cell lung cancer. *Clin Lung Cancer* 2001; 2:229–233.
  173. Everitt S, Schneider-Kolsky M, Yuen K, et al. Dose escalation of radical radiation therapy in non-small-cell lung cancer using positron emission tomography/computed tomography-defined target volumes: are class solutions obsolete? *J Med Imaging Radiat Oncol* 2008; 52:168–177.
  174. Klopp AH, Chang JY, Tucker SL, et al. Intrathoracic patterns of failure for non-small-cell lung cancer with positron-emission tomography/computed tomography-defined target delineation. *Int J Radiat Oncol Biol Phys* 2007; 69:1409–1416.
  175. De Ruyscher D, Wanders S, van Haren E, et al. Selective mediastinal node irradiation based on FDG-PET scan data in patients with non-small-cell lung cancer: a prospective clinical study. *Int J Radiat Oncol Biol Phys* 2005; 62:988–994.
  176. Neicu T, Berbeco R, Wolfgang J, et al. Synchronized moving aperture radiation therapy (SMART): improvement of breathing pattern reproducibility using respiratory coaching. *Phys Med Biol* 2006; 51:617–636.
  177. Yaremko B, Riauka T, Robinson D, et al. Thresholding in PET images of static and moving targets. *Phys Med Biol* 2005; 50:5969–5982.
  178. Nestle U, Kremp S, Schaefer-Schuler A, et al. Comparison of different methods for delineation of 18F-FDG PET-positive tissue for target volume definition in radiotherapy of patients with non-small cell lung cancer. *J Nucl Med* 2005; 6:1342–1348.
  179. Belhassen S, Lina Fuentes CS, Dekker A, et al. Comparative methods for 18F-FDG PET-based delineation of target volumes in non-small-cell lung cancer [abstract]. *J Nucl Med* 2009; 50 In press.
  180. van Westreenen HL, Westerterp M, Bossuyt PMM, et al. Systematic review of the staging performance of 18F-Fluorodeoxyglucose positron emission tomography in esophageal cancer. *J Clin Oncol* 2004; 22:3805–3812.
  181. Vrieze O, Haustermans K, De Wever W, et al. Is there a role for FGD-PET in radiotherapy planning in esophageal carcinoma? *Radiother Oncol* 2004; 73:269–275.
  182. Vinjamuri S, Ray S. Added value of PET and PET-CT in oesophageal cancer: a review of current practice. *Nucl Med Commun* 2008; 29:4–10.
  183. van Vliet EP, Heijenbrok-Kal MH, Hunink MG, et al. Staging investigations for oesophageal cancer: a meta-analysis. *Br J Cancer* 2008; 98:547–557.
  184. Bruzzi JF, Munden RF, Truong MT, Marom EM, Sabloff BS, Gladish GW, et al. PET/CT of esophageal cancer: its role in clinical management. *Radiographics* 2007; 27:1635–1652.
  185. Narayan K, Hicks RJ, Jobling T, et al. A comparison of MRI and PET scanning in surgically staged loco-regionally advanced cervical cancer: potential impact on treatment. *Int J Gynecol Cancer* 2001; 11:263–271.
  186. Khan N, Oriuchi N, Yoshizaki A, et al. Diagnostic accuracy of FDG PET imaging for the detection of recurrent or metastatic gynecologic cancer. *Ann Nucl Med* 2005; 19:137–145.
  187. Grisar D, Almog B, Levine C, et al. The diagnostic accuracy of 18F-fluorodeoxyglucose PET/CT in patients with gynecological malignancies. *Gynecol Oncol* 2004; 94:680–684.
  188. Nakamoto Y, Saga T, Fujii S. Positron emission tomography application for gynecologic tumors. *Int J Gynecol Cancer* 2005; 15:701–709.
  189. Esthappen J, Mutic S, Malyapa RS, et al. Treatment planning guidelines regarding the use of CT/PET-guided IMRT for cervical carcinoma with positive paraaortic lymph nodes. *Int J Radiat Oncol Biol Phys* 2004; 58:1289–1297.
  190. Mutic S, Grigsby PW, Low DA, et al. PET-guided three-dimensional treatment planning of intracavitary gynecologic implants. *Int J Radiat Oncol Biol Phys* 2002; 52:1104–1110.
  191. Mutic S, Malyapa RS, Grigsby PW, et al. PET-guided IMRT for cervical carcinoma with positive para-aortic lymph nodes—a dose-escalation treatment planning study. *Int J Radiat Oncol Biol Phys* 2003; 55:28–35.
  192. Kantorova I, Lipska L, Belohlavek O, et al. Routine (18F)-FDG PET preoperative staging of colorectal cancer: comparison with conventional staging and its impact on treatment decision making. *J Nucl Med* 2003; 44:1784–1788.
  193. Anderson C, Koshy M, Staley C, et al. PET-CT fusion in radiation management of patients with anorectal tumors. *Int J Radiat Oncol Biol Phys* 2007; 69:155–162.
  194. Podoloff DA, Macapinlac HA. PET and PET/CT in management of the lymphomas. *Radiol Clin North Am* 2007; 45:689–696.
  195. Juweid ME, Stroobants S, Hoekstra OS, et al. Use of positron emission tomography for response assessment of lymphoma: consensus of the imaging subcommittee of International harmonization project in lymphoma. *J Clin Oncol* 2007; 25:571–578.
  196. Lee YK, Cook G, Flower MA, et al. Addition of 18F-FDG-PET scans to radiotherapy planning of thoracic lymphoma. *Radiother Oncol* 2004; 73:277–283.
  197. Girinsky T, Ghalibafian M, Bonniaud G, et al. Is FDG-PET scan in patients with early stage Hodgkin lymphoma of any value in the implementation of the involved-node radiotherapy concept and dose painting? *Radiother Oncol* 2007; 85:178–186.

198. Hutchings M, Loft A, Hansen M, et al. Clinical impact of FDG-PET/CT in the planning of radiotherapy for early-stage Hodgkin lymphoma. *Eur J Haematol* 2007; 78:206–212.
199. Veronesi U, De Cicco C, Galimberti V, et al. A comparative study on the value of FDG-PET and sentinel node biopsy to identify occult axillary metastases. *Ann Oncol* 2007; 18:473–478.
200. Barranger E, Grahek D, Antoine M, et al. Evaluation of fluorodeoxyglucose positron emission tomography in the detection of axillary lymph node metastases in patients with early-stage breast cancer. *Ann Surg Oncol* 2003; 10:622–627.
201. Zornoza G, Garcia-Velloso MJ, Sola J, et al. 18F-FDG PET complemented with sentinel lymph node biopsy in the detection of axillary involvement in breast cancer. *Eur J Surg Oncol* 2004; 30:15–19.
202. Lovrics PJ, Chen V, Coates G, et al. A prospective evaluation of positron emission tomography scanning, sentinel lymph node biopsy, and standard axillary dissection for axillary staging in patients with early stage breast cancer. *Ann Surg Oncol* 2004; 11:846–853.
203. Cardillo A, De Cicco C, Paganelli G, et al. Role of fluorodeoxyglucose positron emission tomography in the staging of patients with breast cancer candidate to surgery. *Ann Oncol* 2007; 18:394–395.
204. Gil-Rendo A, Zornoza G, Garcia-Velloso MJ, et al. Fluorodeoxyglucose positron emission tomography with sentinel lymph node biopsy for evaluation of axillary involvement in breast cancer. *Br J Surg* 2006; 93:707–712.
205. Mavi A, Urhan M, Yu JQ, et al. Dual time point 18F-FDG PET imaging detects breast cancer with high sensitivity and correlates well with histologic subtypes. *J Nucl Med* 2006; 47:1440–1446.
206. Heusner TA, Freudenberg LS, Kuehl H, et al. Whole-body PET/CT-mammography for staging breast cancer: initial results. *Br J Radiol* 2008; 81:743–748.
207. Heusner TA, Kuemmel S, Umutlu L, et al. Breast cancer staging in a single session: whole-body PET/CT mammography. *J Nucl Med* 2008; 49:1215–1222.
208. Bral S, Vinh-Hung V, Everaert H, et al. The use of molecular imaging to evaluate radiation fields in the adjuvant setting of breast cancer: a feasibility study. *Strahlenther Onkol* 2008; 184:100–104.
209. Doshi NK, Silverman RW, Shao Y, et al. maxPET, a dedicated mammary and axillary region PET imaging system for breast cancer. *IEEE Trans Nucl Sci* 2001; 48:811–815.
210. Levin CS, Foudray AM, Habte F. Impact of high energy resolution detectors on the performance of a PET system dedicated to breast cancer imaging. *Phys Med* 2006; 21(Suppl 1):28–34.
211. Abreu MC, et al. Clear-PEM: a PET imaging system dedicated to breast cancer diagnostics. *Nucl Instr Meth A* 2007; 571:81–84.
212. Surti S, Karp JS. Design considerations for a limited angle, dedicated breast, TOF PET scanner. *Phys Med Biol* 2008; 53:2911–2921.
213. Murthy K, Aznar M, Thompson CJ, et al. Results of preliminary clinical trials of the positron emission mammography system PEM-I: a dedicated breast imaging system producing glucose metabolic images using FDG. *J Nucl Med* 2000; 41:1851–1858.
214. Rosen EL, Turkington TG, Soo MS, et al. Detection of primary breast carcinoma with a dedicated, large-field-of-view FDG PET mammography device: initial experience. *Radiology* 2005; 234:527–534.
215. Raylman RR, Majewski S, Smith MF, et al. The positron emission mammography/tomography breast imaging and biopsy system (PEM/PET): design, construction and phantom-based measurements. *Phys Med Biol* 2008; 53:637–653.
216. Zangheri B, Messa C, Picchio M, et al. PET/CT and breast cancer. *Eur J Nuc Med Mol Imaging* 2004; 31:S135–S142.
217. Lindfors KK, Boone JM, Nelson TR, et al. Dedicated breast CT: initial clinical experience. *Radiology* 2008; 246:725–733.
218. Liang H, Yang Y, Yang K, et al. A microPET/CT system for in vivo small animal imaging. *Phys Med Biol* 2007; 52:3881–3894.
219. Grosu AL, Pieri M, Weber WA, et al. Positron emission tomography for radiation treatment planning. *Strahlenther Onkol* 2005; 181:483–499.
220. Koch CJ, Evans SM. Non-invasive PET and SPECT imaging of tissue hypoxia using isotopically labeled 2-nitroimidazoles. *Adv Exp Med Biol* 2003; 510:285–292.
221. Beck R, Roper B, Carlsen JM, et al. Pretreatment 18F-FAZA PET predicts success of hypoxia-directed radiochemotherapy using tirapazamine. *J Nucl Med* 2007; 48:973–980.
222. Sorger D, Patt M, Kumar P, et al. [18F]Fluoroazomycinarabino-furanoside (18FAZA) and [18F]Fluoromisonidazole (18FMISO): a comparative study of their selective uptake in hypoxic cells and PET imaging in experimental rat tumors. *Nucl Med Biol* 2003; 30:317–326.
223. Tanaka T, Furukawa T, Fujieda S, et al. Double-tracer autoradiography with Cu-ATSM/FDG and immunohistochemical interpretation in four different mouse implanted tumor models. *Nucl Med Biol* 2006; 33:743–750.
224. Rischin D, Hicks RJ, Fisher R, et al. Prognostic significance of [18F]-misonidazole positron emission tomography-detected tumor hypoxia in patients with advanced head and neck cancer randomly assigned to chemoradiation with or without tirapazamine: a substudy of Trans-Tasman Radiation Oncology Group Study 98.02. *J Clin Oncol* 2006; 24:2098–2104.
225. Thorwarth D, Eschmann SM, Scheiderbauer J, et al. Kinetic analysis of dynamic 18F-fluoromisonidazole PET correlates with radiation treatment outcome in head-and-neck cancer. *BMC Cancer* 2005; 5:152.
226. Lee NY, Mechalakos JG, Nehmeh S, et al. Fluorine-18-labeled fluoromisonidazole positron emission and computed tomography-guided intensity-modulated radiotherapy for head and neck cancer: a feasibility study. *Int J Radiat Oncol Biol Phys* 2008; 70:2–13.
227. Lin Z, Mechalakos J, Nehmeh S, et al. The influence of changes in tumor hypoxia on dose-painting treatment plans based on (18)F-FMISO positron emission tomography. *Int J Radiat Oncol Biol Phys* 2008; 70:1219–1228.
228. Eschmann SM, Paulsen F, Reimold M, et al. Prognostic impact of hypoxia imaging with 18F-misonidazole PET in non-small cell lung cancer and head and neck cancer before radiotherapy. *J Nucl Med* 2005; 46:253–260.
229. Lawrentschuk N, Poon AM, Foo SS, et al. Assessing regional hypoxia in human renal tumours using 18F-fluoromisonidazole positron emission tomography. *BJU Int* 2005; 96:540–546.
230. Rajendran JG, Wilson DC, Conrad EU, et al. [(18)F]FMISO and [(18)F]FDG PET imaging in soft tissue sarcomas: correlation of hypoxia, metabolism and VEGF expression. *Eur J Nucl Med Mol Imaging* 2003; 30:695–704.
231. Eschmann SM, Paulsen F, Bedeshem C, et al. Hypoxia-imaging with (18)F-Misonidazole and PET: changes of kinetics during radiotherapy of head-and-neck cancer. *Radiother Oncol* 2007; 83:406–410.
232. Dolbier WR Jr, Li AR, Koch CJ, et al. [18F]-EF5, a marker for PET detection of hypoxia: synthesis of precursor and a new fluorination procedure. *Appl Radiat Isot* 2001; 54:73–80.
233. Komar G, Seppanen M, Eskola O, et al. 18F-EF5: a new PET tracer for imaging hypoxia in head and neck cancer. *J Nucl Med* 2008; 49:1944–1951.
234. Evans S, Hahn S, Judy K, et al. 18F EF5 PET imaging with immunohistochemical validation in patients with brain lesions [abstract]. *Int J Rad Oncol Biol Phys* 2006; 66:S248.
235. Reinhardt MJ, Kubota K, Yamada S, et al. Assessment of cancer recurrence in residual tumors after fractionated radiotherapy: a comparison of fluorodeoxyglucose, L-methionine and thymidine. *J Nucl Med* 1997; 38:280–287.
236. Grosu AL, Weber WA, Riedel E, et al. L-(methyl-11C) methionine positron emission tomography for target delineation in resected high-grade gliomas before radiotherapy. *Int J Radiat Oncol Biol Phys* 2005; 63:64–74.
237. Terakawa Y, Tsuyuguchi N, Iwai Y, et al. Diagnostic accuracy of 11C-methionine PET for differentiation of recurrent brain tumors from radiation necrosis after radiotherapy. *J Nucl Med* 2008; 49:694–699.
238. Singhal T, Narayanan TK, Jain V, et al. 11C-L-methionine positron emission tomography in the clinical management of cerebral gliomas. *Mol Imaging Biol* 2008; 10:1–18.
239. Nariai T, Tanaka Y, Wakimoto H, et al. Usefulness of L-[methyl-11C] methionine-positron emission tomography as a biological monitoring tool in the treatment of glioma. *J Neurosurg* 2005; 103:498–507.
240. Rachinger W, Goetz C, Popperl G, et al. Positron emission tomography with O-(2-[18F]fluoroethyl)-L-tyrosine versus magnetic resonance

- imaging in the diagnosis of recurrent gliomas. *Neurosurgery* 2005; 57: 505–511.
241. Astner ST, Dobrei-Ciuchendea M, Essler M, et al. Effect of (11)C-methionine-positron emission tomography on gross tumor volume delineation in stereotactic radiotherapy of skull base meningiomas. *Int J Radiat Oncol Biol Phys* 2008; 72:1161–1167.
  242. Grosu AL, Lachner R, Wiedenmann N, et al. Validation of a method for automatic image fusion (BrainLAB System) of CT data and 11C-methionine-PET data for stereotactic radiotherapy using a LINAC: first clinical experience. *Int J Radiat Oncol Biol Phys* 2003; 56:1450–1463.
  243. Grosu AL, Weber WA, Franz M, et al. Reirradiation of recurrent high-grade gliomas using amino acid PET (SPECT)/CT/MRI image fusion to determine gross tumor volume for stereotactic fractionated radiotherapy. *Int J Radiat Oncol Biol Phys* 2005; 63:511–519.
  244. Plotkin M, Gneveckow U, Meier-Hauff K, et al. 18F-FET PET for planning of thermotherapy using magnetic nanoparticles in recurrent glioblastoma. *Int J Hyperthermia* 2006; 22:319–325.
  245. Levivier M, Massager N, Wikler D, et al. Integration of functional imaging in radiosurgery: the example of PET scan. *Prog Neurol Surg* 2007; 20: 68–81.
  246. Mahasittiwat P, Mizoe JE, Hasegawa A, et al. I-[METHYL-(11)C] methionine positron emission tomography for target delineation in malignant gliomas: impact on results of carbon ion radiotherapy. *Int J Radiat Oncol Biol Phys* 2008; 70:515–522.
  247. Miwa K, Matsuo M, Shinoda J, et al. Simultaneous integrated boost technique by helical tomotherapy for the treatment of glioblastoma multiforme with (11)C-methionine PET: report of three cases. *J Neuro-oncol* 2008; 87:333–339.
  248. Tang BN, Levivier M, Heures M, et al. 11C-methionine PET for the diagnosis and management of recurrent pituitary adenomas. *Eur J Nucl Med Mol Imaging* 2006; 33:169–178.
  249. Veas H, Senthamizchelvan S, Miralbell R, et al. Assessment of various strategies for 18F-FET PET-guided delineation of target volumes in high-grade glioma patients. *Eur J Nucl Med Mol Imaging* 2009; 36: 182–193.
  250. Weber DC, Zilli T, Buchegger F, et al. [(18)F]Fluoroethyltyrosine-positron emission tomography-guided radiotherapy for high-grade glioma. *Radiat Oncol* 2008; 3:44.
  251. de Jong IJ, Pruim J, Elsinga PH, et al. 11C-choline positron emission tomography for the evaluation after treatment of localized prostate cancer. *Eur Urol* 2003; 44:32–38; discussion 38–39.
  252. Heinisch M, Dirisamer A, Loidl W, et al. Positron emission tomography/computed tomography with F-18-fluorocholine for restaging of prostate cancer patients: meaningful at PSA < 5 ng/ml? *Mol Imaging Biol* 2006; 8: 43–48.
  253. Picchio M, Messa C, Landoni C, et al. Value of [11C]choline-positron emission tomography for re-staging prostate cancer: a comparison with [18F]fluorodeoxyglucose-positron emission tomography. *J Urol* 2003; 169:1337–1340.
  254. Reske SN, Blumstein NM, Glatting G. [(11)C]choline PET/CT imaging in occult local relapse of prostate cancer after radical prostatectomy. *Eur J Nucl Med Mol Imaging* 2008; 35:9–17.
  255. Veas H, Buchegger F, Albrecht S, et al. 18F-choline and/or 11C-acetate positron emission tomography: detection of residual or progressive subclinical disease at very low prostate-specific antigen values (<1 ng/mL) after radical prostatectomy. *BJU Int* 2007; 99:1415–1420.
  256. Steiner C, Veas H, Zaidi H, et al. Three-phase 18F-fluorocholine PET/CT in the evaluation of prostate cancer recurrence. *Nuklearmedizin* 2009; 48:1–9.
  257. Ciernik IF, Brown DW, Schmid D, et al. 3D-segmentation of the 18F-choline PET signal for target volume definition in radiation therapy of the prostate. *Technol Cancer Res Treat* 2007; 6:23–30.
  258. Picozzi P, Rizzo G, Landoni C, et al. A simplified method to integrate metabolic images in stereotactic procedures using a PET/CT scanner. *Stereotact Funct Neurosurg* 2005; 83:208–212.
  259. Rickhey M, Bogner L. Application of the inverse Monte Carlo treatment planning system IKO for an inhomogeneous dose prescription in the sense of dose painting. *Z Med Phys* 2006; 16:307–312.
  260. Sugiyama M, Sakahara H, Sato K, et al. Evaluation of 3'-deoxy-3'-18F-fluorothymidine for monitoring tumor response to radiotherapy and photodynamic therapy in mice. *J Nucl Med* 2004; 45:1754–1758.
  261. Gabriel M, Decristoforo C, Kendler D, et al. 68Ga-DOTA-Tyr3-octreotide PET in neuroendocrine tumors: comparison with somatostatin receptor scintigraphy and CT. *J Nucl Med* 2007; 48:508–518.
  262. Milker-Zabel S, Zabel-du Bois A, Henze M, et al. Improved target volume definition for fractionated stereotactic radiotherapy in patients with intracranial meningiomas by correlation of CT, MRI, and [68Ga]-DOTATOC-PET. *Int J Radiat Oncol Biol Phys* 2006; 65:222–227.
  263. Austin-Seymour M, Chen GT, Rosenman J, et al. Tumor and target delineation: current research and future challenges. *Int J Radiat Oncol Biol Phys* 1995; 33:1041–1052.
  264. Van Hoe L, Haven F, Bellon E, et al. Factors influencing the accuracy of volume measurements in spiral CT: a phantom study. *J Comput Assist Tomogr* 1997; 21:332–338.
  265. Bowden P, Fisher R, Mac Manus M, et al. Measurement of lung tumor volumes using three-dimensional computer planning software. *Int J Radiat Oncol Biol Phys* 2002; 53:566–573.
  266. Senan S, Chapet O, Lagerwaard FJ, et al. Defining target volumes for non-small cell lung carcinoma. *Semin Radiat Oncol* 2004; 14:308–314.
  267. Chaney E, Ibbott G, Hendee WR. Methods for image segmentation should be standardized and calibrated. *Med Phys* 2005; 32:3507–3510.
  268. Evans PM. Anatomical imaging for radiotherapy. *Phys Med Biol* 2008; 53:R151–R191.
  269. Rasch C, Barillot I, Remeijer P, et al. Definition of the prostate in CT and MRI: a multi-observer study. *Int J Rad Oncol Biol Phys* 1999; 43:57–66.
  270. Khoo VS, Adams EJ, Saran F, et al. A comparison of clinical target volumes determined by CT and MRI for the radiotherapy planning of base of skull meningiomas. *Int J Rad Oncol Biol Phys* 2000; 46: 1309–1317.
  271. Lee YK, Bollet M, Charles-Edwards G, et al. Radiotherapy treatment planning of prostate cancer using magnetic resonance imaging alone. *Radiation Oncol* 2003; 66:203–216.
  272. Chen L, Price J, Robert A, et al. MRI-based treatment planning for radiotherapy: Dosimetric verification for prostate IMRT. *Int J Rad Oncol Biol Phys* 2004; 60:636–647.
  273. Schinagl DA, Kaanders JH, Oyen WJ. From anatomical to biological target volumes: the role of PET in radiation treatment planning. *Cancer Imaging* 2006; 6:S107–S116.
  274. Ashamalla H, Guirguis A, Bieniek E, et al. The impact of positron emission tomography/computed tomography in edge delineation of gross tumor volume for head and neck cancers. *Int J Radiat Oncol Biol Phys* 2007; 68:388–395.
  275. Newbold K, Partridge M, Cook G, et al. Advanced imaging applied to radiotherapy planning in head and neck cancer: a clinical review. *Br J Radiol* 2006; 79:554–561.
  276. Lavrenkov K, Partridge M, Cook G, et al. Positron emission tomography for target volume definition in the treatment of non-small cell lung cancer. *Radiation Oncol* 2005; 77:1–4.
  277. Ford EC, Kinahan PE, Hanlon L, et al. Tumor delineation using PET in head and neck cancers: Threshold contouring and lesion volumes. *Med Phys* 2006; 33:4280–4288.
  278. Ahn PH, Garg MK. Positron emission tomography/computed tomography for target delineation in head and neck cancers. *Semin Nucl Med* 2008; 38:141–148.
  279. Zaidi H. Medical image segmentation: Quo Vadis. *Comput Meth Prog Biomed* 2006; 84:63–67.
  280. Boudraa A, Zaidi H. Image segmentation techniques in nuclear medicine imaging. In: Zaidi H, ed. *Quantitative analysis of nuclear medicine images*. New York: Springer, 2006; 308–357.
  281. Erdi Y, Mawlawi O, Larson S, et al. Segmentation of lung lesion volume by adaptive positron emission tomography image thresholding. Radioimmunodetection and radioimmunotherapy of cancer. Princeton, NJ: American Cancer Society, 1997: 2505–2509.
  282. Daisne JF, Sibomana M, Bol A, et al. Tri-dimensional automatic segmentation of PET volumes based on measured source-to-background ratios: influence of reconstruction algorithms. *Radiation Oncol* 2003; 69:247–250.

283. Drever L, Roa W, McEwan A, et al. Iterative threshold segmentation for PET target volume delineation. *Med Phys* 2007; 34:1253-1265.
284. Schinagl DA, Vogel WV, Hoffmann AL, et al. Comparison of five segmentation tools for 18F-fluoro-deoxy-glucose-positron emission tomography-based target volume definition in head and neck cancer. *Int J Radiat Oncol Biol Phys* 2007; 69:1282-1289.
285. Hatt M, Lamare F, Bousson N, et al. Fuzzy hidden Markov chains segmentation for volume determination and quantitation in PET. *Phys Med Biol* 2007; 52:3467-3491.
286. Montgomery D, Amira A, Zaidi H. Fully automated segmentation of oncological PET volumes using a combined multiscale and statistical model. *Med Phys* 2007; 34:722-736.
287. Drever L, Robinson DM, McEwan A, et al. A local contrast based approach to threshold segmentation for PET target volume delineation. *Med Phys* 2006; 33:1583-1594.
288. Biehli KJ, Kong FM, Dehdashti F, et al. 18F-FDG PET definition of gross tumor volume for radiotherapy of non-small cell lung cancer: is a single standardized uptake value threshold approach appropriate? *J Nucl Med* 2006; 47:1808-1812.
289. Jentzen W, Freudenberg L, Eising EG, et al. Segmentation of PET volumes by iterative image thresholding. *J Nucl Med* 2007; 48:108-114.
290. Ciernik IF, Huser M, Burger C, et al. Automated functional image-guided radiation treatment planning for rectal cancer. *Int J Radiat Oncol Biol Phys* 2005; 62:893-900.
291. Davis JB, Reiner B, Huser M, et al. Assessment of (18)F PET signals for automatic target volume definition in radiotherapy treatment planning. *Radiother Oncol* 2006; 80:43-50.
292. Wong CY, Mahajan P, Yan D. Dynamic threshold for radiation target volume by PET/CT. *J Nucl Med* 2007; 48:849. author reply 847.
293. van Dalen JA, Hoffmann AL, Dicken V, et al. A novel iterative method for lesion delineation and volumetric quantification with FDG PET. *Nucl Med Commun* 2007; 28:485-493.
294. Aristophanous M, Penney BC, Martel MK, et al. A Gaussian mixture model for definition of lung tumor volumes in positron emission tomography. *Med Phys* 2007; 34:4223-4235.
295. Schaefer A, Kremp S, Hellwig D, et al. A contrast-oriented algorithm for FDG-PET-based delineation of tumour volumes for the radiotherapy of lung cancer: derivation from phantom measurements and validation in patient data. *Eur J Nucl Med Mol Imaging* 2008; 35:1989-1999.
296. Breen SL, Publicover J, De Silva S, et al. Intraobserver and interobserver variability in GTV delineation on FDG-PET-CT images of head and neck cancers. *Int J Radiat Oncol Biol Phys* 2007; 68:763-770.
297. Bosmans G, van Baardwijk A, Dekker A, et al. Intra-patient variability of tumor volume and tumor motion during conventionally fractionated radiotherapy for locally advanced non-small-cell lung cancer: a prospective clinical study. *Int J Radiat Oncol Biol Phys* 2006; 66:748-753.
298. Coleman RE, Delbeke D, Guiberteau MJ, et al. Concurrent PET/CT with an integrated imaging system: intersociety dialogue from the joint working group of the American College of Radiology, the Society of Nuclear Medicine, and the Society of Computed Body Tomography and Magnetic Resonance. *J Nucl Med* 2005; 46:1225-1239.
299. Bischof Delaloye A, Carrio I, Cuocolo A, et al. White paper of the European Association of Nuclear Medicine (EANM) and the European Society of Radiology (ESR) on multimodality imaging. *Eur J Nucl Med Mol Imaging* 2007; 34:1147-1151.
300. Graves EE, Quon A, Loo BW Jr. RT\_Image: an open-source tool for investigating PET in radiation oncology. *Technol Cancer Res Treat* 2007; 6:111-121.
301. Jannin P, Fitzpatrick JM, Hawkes DJ, et al. Validation of medical image processing in image-guided therapy. *IEEE Trans Med Imaging* 2002; 21:1445-1449.
302. Tomei S, Reilhac A, Visvikis D, et al. Development of a database of realistic simulated whole body 18F-FDG images for lymphoma. *Proc IEEE Nuclear Science Symposium and Medical Imaging Conference*. Dresden, Germany: IEEE, 2008. 4958-4963.
303. Mamede M, El Fakhri G, Abreu-e-Lima P, et al. Pre-operative estimation of esophageal tumor metabolic length in FDG-PET images with surgical pathology confirmation. *Ann Nucl Med* 2007; 21:553-562.
304. Geets X, Lee J, Bol A, et al. A gradient-based method for segmenting FDG-PET images: methodology and validation. *Eur J Nucl Med Mol Imaging* 2007; 34:1427-1438.
305. Venel Y, Garhi H, de Muret A, et al. Comparaison de six méthodes de segmentation du volume tumoral sur la 18F-FDG TEP-TDM avec le volume de référence anatomopathologique dans les cancers bronchopulmonaires non à petites cellules. *Médecine Nucléaire* 2008; 32:339-353.
306. Drever LA, Roa W, McEwan A, et al. Comparison of three image segmentation techniques for target volume delineation in positron emission tomography. *J Appl Clin Med Phys* 2007; 8:93-109.
307. Visser EP, Philippens MEP, Kienhorst L, et al. Comparison of tumor volumes derived from glucose metabolic rate maps and SUV maps in dynamic 18F-FDG PET. *J Nucl Med* 2008; 49:892-898.
308. Aerts HJ, Bosmans G, van Baardwijk AA, et al. Stability of (18)F-Deoxyglucose uptake locations within tumor during radiotherapy for NSCLC: a prospective study. *Int J Radiat Oncol Biol Phys* 2008; 71:1402-1407.
309. Qiao F, Pan T, Clark J, et al. Joint model of motion and anatomy for PET image reconstruction. *Med Phys* 2007; 34: 426-439.
310. Lamare F, Cresson T, Savean J, et al. Respiratory motion correction for PET oncology applications using affine transformation of list mode data. *Phys Med Biol* 2007; 52:121-140.
311. Rahmim A, Dinelle K, Cheng J-C, et al. Accurate event-driven motion compensation in high-resolution PET incorporating scattered and random events. *IEEE Trans Med Imaging* 2008; 27:1018-1033.
312. Boutchko R, Reutter B, Gullberg G, et al. Correlating motion of internal organs with the displacements of fiducial markers during respiration. *IEEE Nuclear Science Symposium & Medical Imaging Conference*. 19-25 October 2008, Dresden, Germany; 2008, 3641-3642.
313. McQuaid S, Lambrou T, Hutton B. Statistical shape modeling of the diaphragm for application to Rb-82 cardiac PET-CT studies. *IEEE Nuclear Science Symposium & Medical Imaging Conference*. 19-25 October 2008, Dresden, Germany; 2008, 3651-3655.
314. Dey J, Segars W, Pretorius P, et al. Estimation and correction of irregular respiratory motion of the heart in presence of partial angle effects due to amplitude binning in SPECT. *IEEE Nuclear Science Symposium & Medical Imaging Conference*. 19-25 October 2008, Dresden, Germany; 2008, 3656-3662.
315. Bond S, Kadir T, Hamill J, et al. Automatic registration of cardiac PET/CT for attenuation correction. *IEEE Nuclear Science Symposium & Medical Imaging Conference*. 19-25 October 2008, Dresden, Germany; 2008, 5512-5517.
316. Chen S, Tsui B. Accuracy analysis of image-based respiratory motion estimation and compensation in respiratory gated PET reconstruction. *IEEE Nuclear Science Symposium & Medical Imaging Conference*. 19-25 October 2008, Dresden, Germany; 2008, 4292-4295.
317. Lucignani G. Respiratory and cardiac motion correction with 4D PET imaging: shooting at moving targets. *Eur J Nucl Med Mol Imaging* 2009; 36:315-319.
318. Rahmim A, Rousset O, Zaidi H. Strategies for motion tracking and correction in PET. *PET Clin* 2007; 2:251-266.
319. Guido A, Fuccio L, Rombi B, et al. Combined (18)F-FDG-PET/CT imaging in radiotherapy target delineation for head-and-neck cancer. *Int J Radiat Oncol Biol Phys* 2009; 73:759-763.
320. Deantonio L, Beldi D, Gambaro G, et al. FDG-PET/CT imaging for staging and radiotherapy treatment planning of head and neck carcinoma. *Radiat Oncol* 2008; 3:29.
321. Murakami R, Uozumi H, Hirai T, et al. Impact of FDG-PET/CT fused imaging on tumor volume assessment of head-and-neck squamous cell carcinoma: intermethod and interobserver variations. *Acta Radiol* 2008; 49:693-699.
322. Riegel AC, Berson AM, Destian S, et al. Variability of gross tumor volume delineation in head-and-neck cancer using CT and PET/CT fusion. *Int J Radiat Oncol Biol Phys* 2006; 65:726-732.
323. Leong T, Everitt C, Yuen K, et al. A prospective study to evaluate the impact of FDG-PET on CT-based radiotherapy treatment planning for oesophageal cancer. *Radiother Oncol* 2006; 78:254-261.
324. Gondi V, Bradley K, Mehta M, et al. Impact of hybrid fluorodeoxyglucose positron-emission tomography/computed tomography on

- radiotherapy planning in esophageal and non-small-cell lung cancer. *Int J Radiat Oncol Biol Phys* 2007; 67:187–195.
325. Konski A, Doss M, Milestone B, et al. The integration of 18-fluoro-deoxy-glucose positron emission tomography and endoscopic ultrasound in the treatment-planning process for esophageal carcinoma. *Int J Radiat Oncol Biol Phys* 2005; 61:1123–1128.
326. Vesprini D, Ung Y, Dinniwell R, et al. Improving observer variability in target delineation for gastro-oesophageal cancer - the role of (18F)fluoro-2-deoxy-d-glucose positron emission tomography/computed tomography. *Clin Oncol (R Coll Radiol)* 2008; 20:631–638.
327. Yu HM, Liu YF, Hou M, et al. Evaluation of gross tumor size using CT, (18F)-FDG PET, integrated (18F)-FDG PET/CT and pathological analysis in non-small cell lung cancer. *Eur J Radiol*. In press.
328. van Der Wel A, Nijsten S, Hochstenbag M, et al. Increased therapeutic ratio by 18FDG-PET CT planning in patients with clinical CT stage N2-N3M0 non-small-cell lung cancer: a modeling study. *Int J Radiat Oncol Biol Phys* 2005; 61:649–655.
329. Ceresoli GL, Cattaneo GM, Castellone P, et al. Role of computed tomography and [(18F)] fluorodeoxyglucose positron emission tomography image fusion in conformal radiotherapy of non-small cell lung cancer: a comparison with standard techniques with and without elective nodal irradiation. *Tumori* 2007; 93:88–96.
330. Ford EC, Lavelly WC, Frassica DA, et al. Comparison of FDG-PET/CT and CT for delineation of lumpectomy cavity for partial breast irradiation. *Int J Radiat Oncol Biol Phys* 2008; 71:595–602.
331. Dolezelova H, Slampa P, Ondrova B, et al. The impact of PET with 18FDG in radiotherapy treatment planning and in the prediction in patients with cervix carcinoma: results of pilot study. *Neoplasma* 2008; 55:437–441.
332. Lin LL, Mutic S, Low DA, et al. Adaptive brachytherapy treatment planning for cervical cancer using FDG-PET. *Int J Rad Oncol Biol Phys* 2007; 67:91–96.
333. Bassi MC, Turri L, Sacchetti G, et al. FDG-PET/CT imaging for staging and target volume delineation in preoperative conformal radiotherapy of rectal cancer. *Int J Radiat Oncol Biol Phys* 2008; 70:1423–1426.
334. Dehdashti F, Grigsby PW, Mintun MA, et al. Assessing tumor hypoxia in cervical cancer by positron emission tomography with 60Cu-ATSM: relationship to therapeutic response—a preliminary report. *Int J Radiat Oncol Biol Phys* 2003; 55:1233–1238.
335. Popperl G, Gotz C, Rachinger W, et al. Serial O-(2-[(18F)]fluoroethyl)-L-tyrosine PET for monitoring the effects of intracavitary radioimmunotherapy in patients with malignant glioma. *Eur J Nucl Med Mol Imaging* 2006; 33:792–800.